JGR Earth Surface

RESEARCH ARTICLE
10.1029/2022JF006975

The Flocculation State of Mud in the Lowermost Freshwater Reaches of the Mississippi River: Spatial Distribution of Sizes, Seasonal Changes, and Their Impact on Vertical Concentration Profiles

Ryan Osborn[1,2], Kieran B. J. Dunne[3], Thomas Ashley[1,4], Jeffrey A. Nittrouer[5], and Kyle Strom[1]

[1]Civil and Environmental Engineering, Virginia Tech, Blacksburg, VA, USA, [2]Now at U.S. Department of Agriculture, Natural Resources Conservation Service, Boise, ID, USA, [3]Division of Geological and Planetary Sciences, California Institute of Technology, Pasadena, CA, USA, [4]Now at U.S. Bureau of Reclamation, Boulder City, NV, USA, [5]Department of Geosciences, Texas Tech University, Lubbock, TX, USA

Key Points:

- Mud in the Mississippi is flocculated in freshwater reaches, and floc sizes change little in the lateral or vertical direction at a station
- All else being equal, flocs are larger during the summer than they are during the winter
- Measured floc sizes can explain stratification in mud concentration profiles in some, but not all, instances

Correspondence to:
K. Strom,
strom@vt.edu

Citation:
Osborn, R., Dunne, K. B. J., Ashley, T., Nittrouer, J. A., & Strom, K. (2023). The flocculation state of mud in the lowermost freshwater reaches of the Mississippi River: Spatial distribution of sizes, seasonal changes, and their impact on vertical concentration profiles. *Journal of Geophysical Research: Earth Surface*, *128*, e2022JF006975. https://doi.org/10.1029/2022JF006975

Received 21 OCT 2022
Accepted 14 JUN 2023

Abstract We use in situ measurements of suspended mud to assess the flocculation state of the lowermost freshwater reaches of the Mississippi River. The goal of the study was to assess the flocculation state of the mud in the absence of seawater, the spatial distribution of floc sizes within the river, and to look for seasonal differences between summer and winter. We also examine whether measured floc sizes can explain observed vertical distributions of mud concentration through a Rouse profile analysis. Data were collected at the same locations during summer and winter at similar discharges and suspended sediment concentrations. Measurements showed that the mud in both seasons was flocculated and that the floc size could reasonably be represented by a cross-sectional averaged value as sizes varied little over the flow depth or laterally across the river at a given station. Depth-averaged floc sizes ranged from 75 to 200 microns and increased slightly moving downriver as turbulence levels dropped. On average, flocs were 40 microns larger during summer than in winter, likely due to enhanced microbial activity associated with warmer water. Floc size appeared to explain vertical variations in mud concentration profiles when the bed was predominately composed of sand. Average mud settling velocities for these cases ranged from 0.1 to 0.5 mm/s. However, Rouse-estimated settling velocities ranged from 1 to 3 mm/s at two stations during winter where the bed was composed of homogeneous mud. These values exceeded the size-based estimates of settling velocity.

Plain Language Summary Large rivers, such as the Mississippi, carry a substantial amount of fine (muddy) sediment. Where this mud deposits, be it within the river channel itself, the adjacent floodplain, or the coastal zone, depends in part on how fast the mud settles within the water. Mud can exist as a collection of individual particles ranging in size from 1 to 63 microns and/or as aggregates of these particles, known as flocs, whose size, density, and settling speed change with physical, chemical, and biological conditions within the water. Whether mud exists as flocs and how big the flocs are if they do exist in different conditions within a river is difficult to know. The challenges come from the dynamic nature of the aggregate sizes and the difficulty in measuring these flocs within the river itself. In this study, we present data, for the first time, on the flocculation state of mud in the lower freshwater sections of the Mississippi River. Such data aids in understanding where mud may travel to and deposit within the lower Mississippi River Delta and whether or not engineering solutions to land loss, such as diversion structures, can help to promote the emergence of new land.

1. Introduction

Fine muddy sediment with grain sizes less than 63 μm in diameter constitutes a significant fraction of the total sediment load carried by lowland rivers. For example, over the three flood years of 2008–2010, Allison et al. (2012) estimated that 70% of the total sediment load passing Baton Rouge, LA, and over 90% exiting to the Gulf of Mexico was mud. A unique attribute of muddy sediment is its potential to form flocs or aggregates of particles that can change in size, density, and hence settling velocity depending on turbulence conditions in the flow, the amount and type of available sediment, water chemistry, and the level of available organic material and microbial activity (Deng et al., 2021; Eisma, 1986; Horemans et al., 2021; Lefebvre et al., 2012; Mietta et al., 2009; Verney et al., 2009). From a sediment transport perspective, the flocculation potential of mud is

important because particle settling velocity, in conjunction with local concentration, sets sediment deposition rates and can influence the average advective length scale of the suspended material.

Research into the flocculation behavior of muds, and the impact of flocs on sediment transport dynamics, has primarily been investigated within the context of saline coastal and estuarine environments (Eisma, 1986; Gibbs, 1985; Kranck, 1973; Kranck & Milligan, 1992; Manning & Dyer, 2002a). Salt is known to enhance flocculation in laboratory studies of settling in a stagnant column (Kim & Nestmann, 2009; Kranck, 1980), and is often thought to be a controlling factor on flocculation in the field due to the large accumulations of mud in estuarine settings where fresh and saltwater mix and the reduction in the thickness of the electric double layer is known to occur in the presence of cations (Tan et al., 2013); this is true even though many have pointed to organic binders as possibly being the major factor contributing to flocculation of mud in saltwater conditions (e.g., Eisma, 1986; Verney et al., 2009), and hydrodynamic, rather than salt, being responsible for mud accumulations (e.g., Thill et al., 2001). Nevertheless, flocculation of mud is known to be an important factor to consider with respect to mud dynamics in coastal environments (Mehta, 2022; Whitehouse et al., 2000; Winterwerp & van Kesteren, 2004).

Comparatively fewer studies have sought to measure floc properties in freshwater settings or to assess the contribution of flocs to sediment transport dynamics in rivers. The primary reason for this is that saltwater has historically been thought to be necessary to cause significant flocculation of mud. Despite this lingering view, there is ample evidence that mud does exist in aggregate or flocculated form in freshwater fluvial systems. Microscope imaging of sediment captured from freshwater rivers at low (Le et al., 2020), mid (Droppo & Ongley, 1994; Fox et al., 2013), and high latitudes (Droppo et al., 1998) all suggest that material in suspension, and on the bed, are indeed flocculated even in the absence of typical oceanic or estuarine levels of salinity. Various sizing and settling estimates of mud within freshwater suspensions also point to mud existing in some state of aggregation (Bungartz et al., 2006; Marttila & Kløve, 2015; Phillips & Walling, 1999; Woodward & Walling, 2007). Furthermore, recent analyses of vertical concentration profiles from several rivers have shown that mud can indeed be vertically stratified and that flocculation could provide an explanation for the observed behavior (Izquierdo-Ayala et al., 2021; Lamb et al., 2020; Nghiem et al., 2022).

Unlike estuarine sampling where flocs have been imaged and sized in situ with specially designed camera systems (e.g., Cartwright et al., 2011; Fall et al., 2021; Fennessy et al., 1994; Manning & Dyer, 2002b; Markussen et al., 2016), the observation of freshwater aggregates has largely been accomplished through laboratory microscope analysis of samples collected from the water column or bed at some earlier point in time. While this method is not ideal when an understanding of the impact of flocs on sediment transport is desired, it does provide the opportunity to study the composition of the flocs in detail. Such analysis of river water samples has shown the presence of particle aggregates or flocs, and that the flocs are similar in shape and composition to those found in estuaries (Droppo & Ongley, 1994; Fox et al., 2013; Spencer et al., 2021), though they tend to be of size <100 μm. Similar to those in estuaries, freshwater flocs are composed of complex assemblages of inorganic clays and silts, organic detrital material, and particle-attached bacteria and their polymeric byproducts (Droppo et al., 1997; Fall et al., 2021; Liss et al., 1996). In the absence of salt then, it is commonly held that these biofilms and biofilm components are the binding mechanisms for floc assemblages in freshwater settings.

If freshwater flocs are bound together by various organic constituents, then one might expect seasonal or condition-dependent changes in nutrients, temperature, or organic content, in addition to physical conditions such as turbulence or suspended sediment concentration (SSC), to influence floc characteristics. Data are lacking to define fully the nature of freshwater flocs under different physical, chemical, and biological conditions. However, a few studies have indeed observed seasonal or condition-dependent changes in freshwater aggregates' size or shape, and all of them point to some type of alteration in the organics as the underlying driver of the change. For example, Phillips and Walling (1999) observe that mud aggregate size was largest during the spring and summer and that the timing of the observed peak in aggregate size corresponded with the peak in organic content within the bed. Relatedly, Fox et al. (2013) found that aggregates were more irregular and elongated in summer compared to more compact and spherical aggregates in the fall and that the changes in aggregate morphology were highly correlated with seasonal changes in heterotrophic and autotrophic biological activity within the mud deposited on the stream bed.

Changes in organic material type within the water column have also been linked to differences in the potential of the system to generate flocs. For example, Lee et al. (2017) and Lee et al. (2019) found that rain-driven high flows lead to an increase in organic content rich in terrestrial humic substances in the Nakdong River in Korea.

However, the humic-substance-based organics were observed to have a stabilizing effect on the suspended particles thereby suppressing flocculation. Whereas low-flow conditions led to warmer water, algae growth, and associated extracellular polymeric substances (EPS), which enhanced the potential of the water to promote flocculation. Seasonality in estuarine floc sizes or settling properties have also been linked to changes in organic and mineral constituents of the suspension throughout the year (Deng et al., 2021; Fettweis & Baeye, 2015; Fettweis et al., 2022; Mikkelsen et al., 2007; Van der Lee, 2000; Verney et al., 2009).

Identification of flocs in freshwater systems has mostly come through either microscope analysis of aggregates obtained from water column grab or pumped samples or through an indirect measure of size through estimates of settling velocity from a Rouse profile analysis of SSC. In the case of microscope imaging, the material is imaged in conditions different from those the material experienced in its natural setting. This is important because flocs have the ability to change their size as the shearing and mixing level of the fluid changes, for example, going from the river to a sample bottle or sampling pipette to a slide. Furthermore, if the sediment is allowed to settle, it is easier for the sediment to aggregate in the zones of higher concentrations experienced at the bottom of a sampling container from which material might be extracted for imaging. Therefore it is possible that flocs imaged in the lab from field water column samples might not be representative of the flocs as they exist within the turbulent flow of the river.

In addition, the fraction of the mud that exists as flocs, the distribution of floc sizes within the river, and how flocs alter the sediment transport characteristics of the mud in a river is still unclear. For example, the studies of Lamb et al. (2020) and Nghiem et al. (2022) provide compelling evidence that the flocculation of mud is a reasonable explanation for the existence of vertical gradients in mud concentration profiles observed in rivers. Yet, the concentration data used in these studies was not paired with in situ size measurements of the mud, and a direct link between the flocculation state and the sediment transport characteristics has yet to be made. For example, does the flocculation of mud lead to enhanced deposition within the channel and therefore changes in bed morphology and cohesion?

In this field study, we provide novel in situ size observations of the suspended mud in the freshwater reaches of a major river before it enters the saltwater-influenced estuarine portions of the system. The specific questions we seek to answer with the data are: (a) does mud exist in flocculated form before reaching the estuary; (b) if so, how are floc sizes distributed over the vertical (depth), lateral (right to left bank), and longitudinal (up and downstream river stations with slightly different hydraulic conditions); (c) are there seasonal differences in observed flocs between summer and winter; and (d) can measured floc sizes explain measured vertical gradients of mud concentration? To explore these questions, we used the imaging system of Osborn et al. (2021) to obtain direct observations of suspended sediment over the water column during a summer and winter survey from the lowermost freshwater reaches of the Mississippi River. We chose the Mississippi River for this study because it is the terminus of the largest drainage catchment in North America, and because a substantial fraction of its total sediment load is mud (70%–90%). Furthermore, the lowermost freshwater reaches (i.e., the study region for this paper) represent the boundary condition for mud entering the estuarine portions of the main river and adjacent embayments by levee overtopping and through natural and man-made gaps in the levees. Quantifying the aggregation state and settling velocity of mud in this region is key to understanding sediment dispersal and deposition in the region of the delta that faces potential submergence in the face of continued subsidence and sea level rise.

2. Methods

2.1. Overview

The primary data needed to explore our research questions include: in situ measurements of particle and/or floc sizes over the vertical at each sampling location in the river, water column samples of suspended sediment, samples of the bed sediment, and the velocity distribution and shear velocity at the location where profiles of floc size and concentration are measured. Comparison of the data obtained from these samples at different spatial locations, and comparisons between the summer and winter surveys, provide the basis for investigating the flocculation state of mud in the river with respect to location and season (research Questions 1–3). Question 4 is investigated by comparing the settling velocity of the mud flocs calculated from the measured floc sizes to the settling velocity obtained by fitting a Rouse concentration profile to the measured concentration data.

2.2. Background Theory: The Rouse Profile

The Rouse profile (Rouse, 1939) is a particular solution to the following simplified advection-diffusion equation for suspended particulate load,

$$w_s C + \epsilon_s \frac{dC}{dz} = 0 \tag{1}$$

Here C is the SSC, z is the vertical coordinate, and ϵ_s is the vertical sediment diffusivity coefficient used in conjunction with the vertical gradient of C to model vertical advective flux due to time-averaged turbulence. Equation 1 assumes equilibrium transport conditions, that is, that C is locally steady, that velocity and concentration in the down and cross-stream directions are uniform, and that there is no net sediment flux across the free surface. A result of these conditions is that the downward flux of sediment due to settling ($-w_s C$) must be balanced with the upward turbulent diffusive flux ($\epsilon_s dC/dz$).

The Rouse-profile solution to Equation 1 uses a model for ϵ_s based on the 2D shear stress distribution, that is, $\tau = \rho u_*^2(1 - z/H)$ (where ρ is the fluid density, u_* is the shear velocity, and H is the total flow depth), and the argument that suspended sediment diffuses as a result of the eddying motions that also lead to the diffusion of fluid momentum, $\epsilon_s = \nu_T/\beta$, where ν_T is the eddy viscosity or diffusion rate of momentum and β is the Schmidt number which accounts for any differences between mass and momentum diffusion rates. To provide closure, Prandtl's mixing-length theory and the resulting rough-wall log law,

$$\frac{u}{u_*} = \frac{1}{\kappa}\ln\left(30\frac{z}{k_c}\right) \tag{2}$$

can be used in conjunction with the Boussinesq hypotheses, $\tau = \nu_T(du/dz)$, to yield the following equation for ϵ_s:

$$\epsilon_s = \frac{1}{\beta}\kappa u_* z\left(1 - \frac{z}{H}\right) \tag{3}$$

In Equation 2, u is the depth-varying and time-averaged velocity, κ is the von Kàrman constant, and k_c is a composite bed roughness length scale. To account for damping of turbulence due to vertical density stratification, the effective eddy viscosity can be conceived of as the product of the neutral, unstratified eddy viscosity, ν_{T0}, and a factor γ that ranges from $\gamma = 1$ for unstratified conditions to 0 for complete damping, $\nu_T = \gamma\nu_{T0}$. Making use of γ, Equation 3 becomes:

$$\epsilon_s = \frac{\gamma}{\beta}\kappa u_* z\left(1 - \frac{z}{H}\right) \tag{4}$$

Using Equation 4 in the integration of Equation 1 gives rise to the well-known Rouse concentration profile:

$$\frac{C}{C_b} = \left[\frac{(z/H - 1)b}{(b/H - 1)z}\right]^{Z_R} \tag{5}$$

with b being a reference height above the bed (often taken at $z/H = 0.05$), and C_b being the concentration at that reference height, $C(z = b) = C_b$. The exponent Z_R is defined as the Rouse number:

$$Z_R = \frac{\beta w_s}{\gamma\kappa u_*} \tag{6}$$

The Rouse number represents a ratio of downward settling velocity to upward turbulent diffusion velocity of the sediment captured by the ratio of w_s/u_*; the three parameters of γ, β, and κ all represent modifiers on u_* to make it a suitable velocity scale for upward diffusion of sediment due to turbulence. Often β is taken as 1 and $\kappa = 0.41$. γ is also often taken as 1 for simplicity, but it can also be set through additional closure equations to account for vertical damping of turbulence in the presence of density stratification.

For large, low-sloping sand-bed rivers, such as the Mississippi, Wright and Parker (2004a) took the approach of defining a single modifier, α, to account for deviation in the baseline case of $\beta = 1$ and $\gamma = 1$ that could

be caused by sediment induced stratification. In their model, α is equal to γ/β and hence the Rouse number is defined as:

$$Z_R = \frac{w_s}{\alpha \kappa u_*} \tag{7}$$

with α provided through the following empirical fit,

$$\alpha = \begin{cases} 1 - 0.06\left(\frac{C_{5t}}{S_0}\right)^{0.77} & \text{for } \frac{C_{5t}}{S_0} \leq 10 \\ 0.67 - 0.0025\left(\frac{C_{5t}}{S_0}\right) & \text{for } \frac{C_{5t}}{S_0} > 10 \end{cases} \tag{8}$$

In Equation 8, C_{5t} is the volume concentration of suspended sediment at 5% of the flow depth from the bed, and S_0 is the water surface slope. The fit for Equation 8 was developed for C_{5t}/S_0 values ranging from 0 to ≈50 with the majority of the points falling between 0 and 20.

In our particular study, we are interested in fitting Equation 5 to measured mud concentration data for the purpose of obtaining an effective settling velocity for the concentration profile. The data needed to back out a settling velocity estimate in this way include measures of concentration over the vertical, a measure of the friction velocity, and an estimate of α.

2.3. Survey Locations and General River Conditions

Data on the flocculation state of the mud, and outcomes for the Rouse-profile analysis, were produced from the summer and winter sampling surveys on the lower Mississippi River, near the terminus of the river, but upstream of saltwater intrusion. This section of the river was chosen because it maintains a high mud load, has regional geomorphic importance insofar that it is directly connected to the lowland delta region, and because the mud in this section of the river represents the boundary condition for mud entering the estuarine zone of the river and local embayments. Surveys were conducted during summer 2020 and winter 2021. Data were collected at several locations within the river and its distributaries during both surveys. However, in this paper, we focus on data only at three key freshwater locations. These stations are, starting from upstream and progressing downstream, the Bonnet Carré Spillway (BCS) (Figure 1a), the main channel 2 km upriver from the Baptiste Collette distributary, hereinafter referred to as Venice Main Channel (VMC), and at a location within the upstream section of Southwest Pass (SWP) (Figure 1b). During the summer survey, data were collected at two locations along a lateral transect at the BCS and three locations at VMC. The winter survey consisted of data collection at one location within the thalweg at both the BCS and VMC, and a station located approximately 3 km downriver from Head of Passes with SWP just upstream of a saltwater wedge that was being pushed seaward during the survey.

Contextual discharge, water temperature, and average SSC data for the two surveys were acquired from USGS station 07374000 at Baton Rouge, LA (Table 1). During the summer survey (24 June–2 July 2020), the river was on the receding limb of a flow event that reached a peak discharge of just over 28,300 m^3/s before the start of the survey. Over the duration of the summer survey, the discharge dropped from 22,200 on 24 June to 16,480 m^3/s on 02 July. The average daily water temperature during the summer survey was 27.3°C. The winter survey took place from 9 to 14 January 2021. In the five months prior to the survey, discharge did not exceed 13,500 m^3/s. Then, approximately one week before the winter survey, discharge began to increase from 12,000 m^3/s on 2 January 2021, up through the end of the survey period on 14 January 2021. During the survey, discharge ranged from 17,783 on 9 January to 19,737 m^3/s on 14 January. The daily average water temperature during the winter survey was 6.3°C.

Average daily turbidity values are reported from the Baton Rouge station. Paired historic USGS physical water column samples of suspended sediment and measured turbidity in FNU were used to create a calibration equation, $C_{avg} = 2.0(\text{FNU}) + 32.4$ ($R^2 = 0.81$), between turbidity and concentration. Using the calibration equation, SSC was between 100 and 200 mg/L during both surveys with concentration being greater during winter (Table 1).

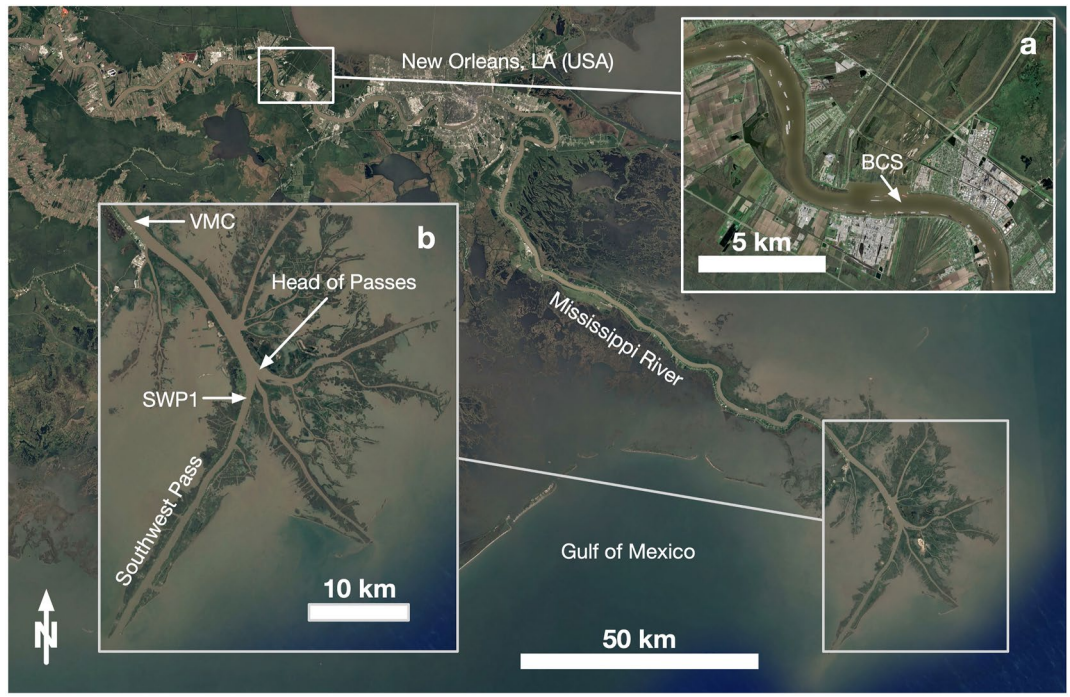

Figure 1. Survey locations. (a) Bonnet Carré Spillway. (b) Mississippi River Delta, including stations Venice Main Channel and SWP1.

2.4. Field Measurements

All sampling and field measurements were made on the river from an 8-m survey vessel (Figure 2). Primary data collected included floc size and concentration measurements over the vertical, water column velocity over the vertical, physical water column samples over the vertical, and bed sediment samples.

Particle and/or floc sizes and concentrations were obtained with the Floc AReA and siZing Instrument (FlocARAZI) imaging system (Osborn et al., 2021). The FlocARAZI was designed to image flocculated suspended sediment in situ over the water column at depths up to 60 m, identify sand within particle data, and estimate mass SSC from image data. During deployment, a live video feed from the camera is transmitted via a Cat6 Ethernet cable to a laptop at the surface where images are saved to the hard drive. A Sontek CastAway CTD is attached to the frame of the FlocARAZI to provide conductivity, temperature, and depth information for each image (Figure 2).

The FlocARAZI system itself consists of a camera, microscope lens, and LED light source situated within a waterproof housing. The camera system has a field of view of 3.7 × 2.8 mm and can resolve particles down to 6 microns. Suspended sediment is allowed to pass freely through a flow-through cell with a gap width of 1.17 mm. Images collected with the system are processed following the image processing routine developed by Keyvani and Strom (2013), with modifications outlined in Osborn et al. (2021). The relevant output from the image processing routine is the particle area in square pixels, which is converted to an equivalent circular diameter. The particle diameter is converted from pixels to microns with 0.925 microns/pixel conversion factor. A processing routine utilizing a trained Support Vector Machine classifier allows for identifying sand particles

Table 1
Discharge, Temperature, and Suspended Sediment Concentration (SSC) at the USGS 07374000 Baton Rouge Station

Survey season	Start date	End date	Q_{avg} (m^3/s)	Q_{start} (m^3/s)	Q_{end} (m^3/s)	H_{avg} (m)	T_{avg} (°C)	C_{avg} (mg/L)[a]
Summer	24 June 2020	02 July 2020	19,073	22,200	16,480	18–23	27.3	126
Winter	09 January 2021	14 January 2021	18,939	17,783	19,737	17–21	6.3	182

[a]Obtained through a calibration between USGS-measured SSC and FNU.

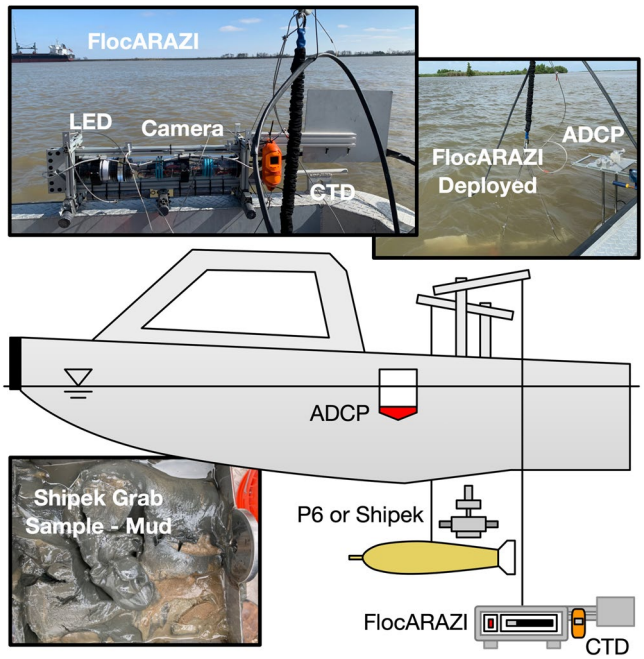

Figure 2. Survey boat schematic with primary sampling instrumentation.

within the full particle data set, providing the means to isolate and analyze the flocculated and silt fraction of suspended sediment separate from the full imaged particle data set.

During deployment of the FlocARAZI, images are collected at a frequency of 2 Hz. With the CTD sampling initiated, the camera system was lowered in 3-m increments from the free surface to the bed. At each increment over the water column, the FlocARAZI position was held steady for 1–2 min to collect approximately 90 images suitable for processing. While the FlocARAZI was deployed, velocity profiles were collected continuously with a Teledyne RiverPro Acoustic Doppler current profiler (ADCP). Velocity profiles were collected at an average sampling rate of 0.47 Hz with 0.69–0.85 m bins in the vertical.

Physical point samples of river water were collected at 5%, 25%, 50%, 75%, and 95% of the flow depth at each station using a USGS isokinetic P6 sampler (Figure 2). Collecting water samples consisted of holding the boat position steady, lowering the P6 to the predetermined depth, and opening the solenoid valve to fill a 1 L sample bottle. The solenoid is opened for a period of time ranging from 10 to 60 s depending on current speeds, allowing for the sample bottle to fill to approximately 75% capacity, ensuring the sample bottle is not overfilled during sampling. Water samples were filtered on-site with 1 μm glass fiber filters and the liquid volume of the sample was recorded. Once back in the lab, filtered water samples were allowed to dry in an oven at 80°C for 24 hr. The sample and filter were then weighed and the mass of the filter was subtracted to obtain the mass of the sample and hence the suspended mass concentration for each sample. Additional P6 samples were used to measure the disaggregated size distribution of the suspended material. These samples were dosed with sodium hexametaphosphate and sonicated prior to sizing with a LISST-Portable XR. Data from the LISST-Portable XR were only used for the purposes of obtaining estimates of the disaggregated particle sizes. The LISST was not used to size particles in suspension or from the raw water column samples due to the limitations associated with using a LISST for large, low-density, irregularly shaped particles, and aggregates (Mikkelsen et al., 2005; Smith & Friedrichs, 2011).

Bed material samples were collected at each station with a Shipek grab sampler (Figure 2). Samples were processed by first mixing the sediment until homogeneous. A subsample of the homogenized sample was then wet sieved with a No. 230 (63 μm) mesh sieve to separate the fine and coarse sediment. The grain size distribution of the coarse fraction was obtained by sizing with a Retsch Technology Camsizer.

2.5. Analysis Calculations: Settling Velocity Estimate Through Rouse Profile Fit

The Rouse profile analysis includes fitting Equation 5 to the measured concentration profiles using w_s as the fit parameter and then comparing these fit values of w_s to ones predicted from a settling-velocity equation and the measured floc sizes. Data and parameters needed for the fit include the concentration profile data $C = C(z)$, the concentration at a reference height, C_b, a measure of u_* or for the station, and a measure of sediment stratification to account for the effects of turbulence damping, α.

For the analysis, data for $C = C(z)$ was obtained using data from the FlocARAZI following the methods presented in Osborn et al. (2021). For the winter surveys, SSC measurements were collected at all three stations included in the analysis (BCS, VMC, SWP1). For all three stations, the SSC measurements made with the P6 were used to inform the correction factor needed for FlocARAZI SSC measurements. The correction factor for each station was obtained by visually observing the best fit, by trial and error, between the SSC measured with the P6 and those estimated by the FlocARAZI. During the winter survey, a large amount of sand was present in suspension at the BCS. Therefore, the correction factor for the FlocARAZI SSC measurements was obtained by fitting the P6 SSC measurements to the total SSC estimated, including both mud and sand, with the FlocARAZI. Little sand was observed in suspension at the VMC or SWP1 stations during the winter survey, as such, both the SSC measured with the FlocARAZI and P6 water samples are assumed to contain little to no sand. The correction factor

used for the SSC estimates from the summer survey were derived from an average of the correction factors used for the winter survey stations; concentration estimated with the camera using the winter calibration parameters fit within calculated concentrations from the Baton Rouge station (Table 1), resulting in slightly lower concentrations overall in summer relative to winter. For the winter data, the P6 measured SSC at 5% of the flow depth from the bed was used as the reference depth and concentration. For the summer survey, these values were taken as the lowest depth where a SSC measurement was collected.

ADCP velocity data were used to obtain shear-velocity estimates. The method for calculating u_* included taking the average flow velocity, u, at each depth interval against the natural log of the distance from the channel bed, z, fitting a line through the data, and multiplying the slope of the resulting line by $\kappa = 0.41$ (Equation 2). When no bedforms are present, shear velocity calculated using this method was used directly in the Rouse profile calculations. To account for the impact of bedforms, the empirical relation developed by Wright and Parker (2004b) for large, low-sloping sand bed rivers was employed to estimate the non-dimensional skin friction shear stress, τ_{*s}, from which the skin friction velocity driving transport was obtained:

$$\tau_{*s} = 0.05 + 0.7\left(\tau_* \, Fr^{0.7}\right)^{0.8} \tag{9}$$

In Equation 9, τ_* is the total dimensionless bed shear stress, and Fr is the Froude number where $Fr = U/\sqrt{gH}$; where U is the depth-averaged velocity (obtained from ADCP measurements). By definition, the total dimensionless bed shear stress is:

$$\tau_* = \frac{u_*^2}{gR_s d} \tag{10}$$

with the dimensionless skin-friction shear stress, from which the needed skin-friction component of the shear velocity (u_{*s}) is obtained, being:

$$\tau_{*s} = \frac{u_{*s}^2}{gR_s d} \tag{11}$$

In all cases g is the acceleration due to gravity, d is the characteristic grain size, taken here as d_{50}, and R_s is the submerged specific gravity, given by $R_s = (\rho_s - \rho)/\rho$ where ρ_s is the density of the sediment.

The effect of turbulence damping due to sediment stratification was accounted for by Equation 8. To use Equation 8, the volume concentration of sediment at 5% of the flow depth and the water surface slope are needed. C_{t5} was calculated assuming a sediment density of 2,650 kg/m^3 and a water density of 1,000 kg/m^3 in accordance with the method established in Wright and Parker (2004a). Estimates of the water surface slope were obtained from Nittrouer et al. (2011), where the authors present water surface slope measurements obtained upriver from Head of Passes under varying discharge ranges.

With the shear velocity and stratification parameter constrained, the only remaining variable within the Rouse number (Equation 7) is the settling velocity, w_s. The settling velocity was obtained by performing a least squares regression analysis by fitting a Rouse profile to concentration data obtained from the FlocARAZI and physical water samples, allowing the settling velocity to vary.

2.6. Analysis Calculations: Settling Velocity Based on Floc Size

Expected values of w_s based on measured size were calculated using the settling-velocity equation of Ferguson and Church (2004) as modified by Strom and Keyvani (2011) for flocs. The primary Ferguson and Church (2004) equation,

$$w_s = \frac{gR_f d_f^2}{b_1 \nu + b_2 \sqrt{gR_f d_f^3}} \tag{12}$$

is designed to work under both inertial and viscous settling conditions. Key inputs to the model include R_f, the submerged specific gravity of the floc, which is related to floc density as $\rho_f = \rho(R_f + 1)$, and the coefficients b_1 and b_2, which act as calibration coefficients that account for floc shape, permeability, and impacts from drag

Table 2
Measured Hydraulic and Water Quality Parameters

Station	U (m/s)	H (m)	u_* (m/s)	u_{*s} (m/s)	S_0	Bed	C_b (mg/L)	SpC (μS/cm)	S (PSU)
BCS Summer	1.05	23.0	0.094	0.037	1.5E−05	Sand	136	440	0.20
VMC Summer	0.76	18.0	0.063	0.026	6.0E−06	Sand	122	395	0.18
BCS Winter	0.89	20.5	0.098	0.037	2.0E−05	Sand	160	215	0.16
VMC Winter	0.79	18.5	0.05	–	6.0E−06	Mud	268	271	0.19
SWP1 Winter	0.62	17.0	0.04	–	6.0E−06	Mud	484	275	0.19

Note. Water surface slope, S_0, was estimated from Nittrouer et al. (2011).

within the inertial range. ν is the kinematic viscosity of the fluid. Note that setting $b_1 = 18$ and $b_2 = 0$ reduces Equation 12 to Stokes settling.

Average floc density, or R_f, is known to be reasonably described as a decreasing power function of size (Mehta, 2022). One way to model such behavior is to assume that flocs are 3D fractal objects built out of smaller primary particles in a self-similar way (Kranenburg, 1994). Doing so provides a model for R_f that is dependent on the primary particle size, d_p, primary particle submerged specific gravity, R_s, and the 3D fractal dimension, n_f,

$$R_f = R_s\left(\frac{d_f}{d_p}\right)^{n_f-3} \tag{13}$$

Combining Equations 12 and 13 provides a means of estimating floc settling velocity given the size of the floc, the size and density of the primary particles, a fractal dimension, and values for the shape and porosity coefficients b_1 and b_2 (Strom & Keyvani, 2011). Variation in any of the input parameters (d_p, R_s, n_f, b_1, and b_2) for a given fluid viscosity will produce a different predicted settling velocity at a particular floc size; a sensitivity analysis using reasonable variations in these input parameters is provided in Strom and Keyvani (2011). To help constrain the calculations, Strom and Keyvani (2011) fit the model to a wide range of laboratory and field data to obtain best-fit values for b_1, b_2, and n_f using measured settling velocity and floc sizes with assumed primary particle size and $R_s = 1.65$. The best overall correlation between the predicted settling velocity and measured data was produced with model coefficients of $n_f = 2.5$, $b_1 = 100$, and $b_2 = 0$; these model coefficient values have also been shown to yield reasonable estimates of floc settling velocities when w_s is calculated with a site-specific density function (Markussen & Andersen, 2013).

Two comments pertaining to the way in which we estimate floc settling velocity based on flocs size need to be made. First, while flocs are not truly fractal in nature (e.g., Spencer et al., 2021, 2022), we use Equation 13 in our calculation of settling velocity as a pragmatic means of modeling the power-law decay in R_f with d_f in a simple yet physically understandable way. Additionally, because many other studies have also used the approach, it is possible to put reasonable bounds on expected values for the power exponent, n_f.

Second, the model (Equations 12 and 13) will return a single value of w_s for a given d_f, d_p, R_s, n_f, and b_1 and b_2 coefficients even though the density and shape of a floc characterized by a given length scale can vary widely in different natural settings, and even from floc to floc within the same environment as a function of particle composition (e.g., Manning et al., 2010; Markussen & Andersen, 2013). Therefore, one would expect there to be a range of "true" settling velocities for flocs of a given size in the Mississippi River, and that calibration of the model might be required to produce best estimates of the data. However, in the absence of any measured settling velocity or floc density estimates, we use Equations 12 and 13 with $n_f = 2.5$, $b_1 = 100$, and $b_2 = 0$ as a reasonable, first-pass estimate of the settling velocity based on measured floc sizes.

3. Results

3.1. Overview

Depths at all sampling locations ranged from 17 to 25 m with depth-averaged velocities of ≈1 m/s near the BCS and $U \approx 0.75$ m/s at VMC (Table 2); overall, flow conditions at the VMC were less energetic than at the BCS. Salinity was near zero at all stations, uniform over the depth, and very close in absolute reported PSU values to

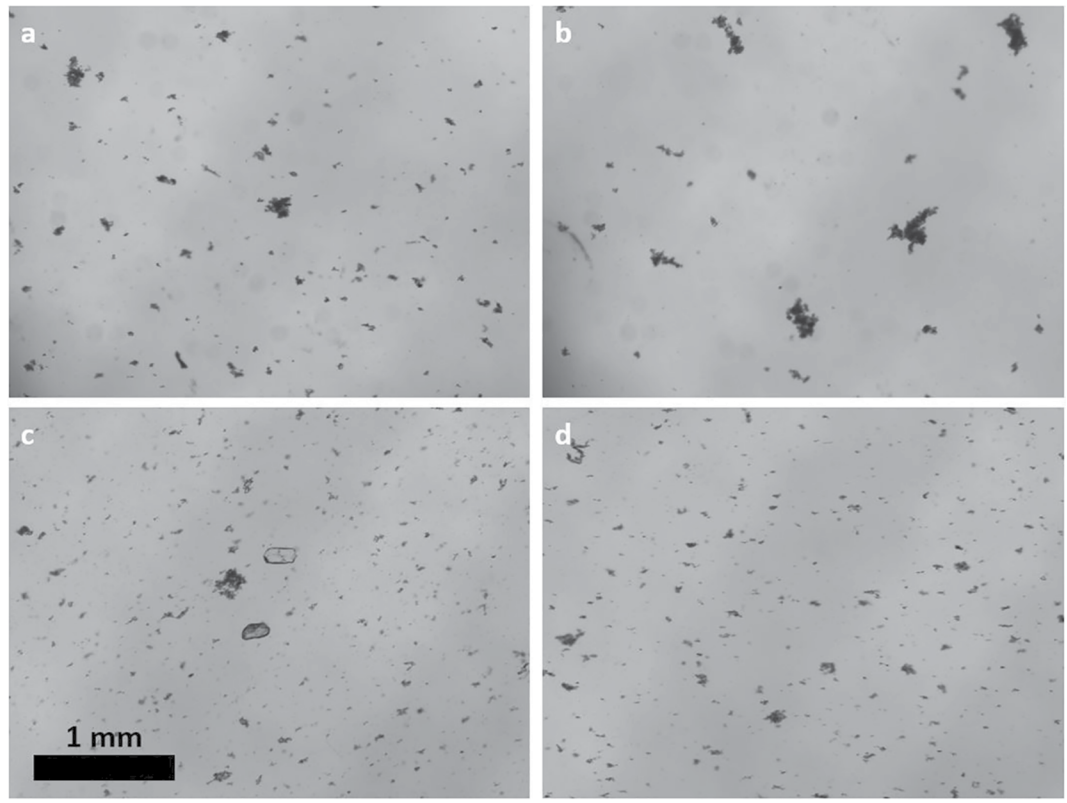

Figure 3. Example images collected during the summer at the (a) Bonnet Carré Spillway (BCS) and (b) Venice Main Channel (VMC), and during the winter at the (c) BCS and (d) VMC. The grains of sand in panel (c) have an equivalent spherical diameter of approximately 160 μm.

the instrument's accuracy (±0.1 PSU). In general, specific conductance was slightly higher during summer than winter by 100–200 μmS/cm. The bed material at the BCS was composed of sand (d_{50} = 0.22 mm) during both the summer and winter surveys, and large definable dunes were observed through the ship's onboard sonar. The bed material at the VCM station during summer was also composed of sand (d_{50} = 0.20 mm) and dunes of notable size were again evident in the ship's sonar. However, during the winter survey, the bed at the VMC station was unconsolidated mud (90.3% of the material was <63 μm) with no evident bedforms (Figure 2); the lack of bedform could be due either to the filling and capping of the bed with a thick mud layer (e.g., Galler & Allison, 2008) or the blanketing of mud in conjunction with transformation to bedforms due to added cohesion (e.g., Parsons et al., 2016). Similar bed composition and morphology were observed downstream at SWP1.

Suspended mud (d < 63 μm) from each station had a disaggregated d_{50} of approximately 6–15 μm. However, in situ images showed that at all sites, suspended mud was flocculated within the river (Figure 3) with a significant fraction of the material existing in aggregates that far exceeded 15 μm. The images also showed that some of the silt in suspension existed as individual free solid particles, but that much of the silt, even up to 63 μm in size, was bound within large floc aggregates similar to Tran and Strom (2017). This was true regardless of season, river station, or depth. This broadly confirms that similar to other rivers (Droppo & Ongley, 1994) and flume studies (Schieber et al., 2007), salty marine water is not necessary for mud in the Mississippi River to exist in flocculated form. Studies such as Galler and Allison (2008) and Lamb et al. (2020) have pointed to the possible role of flocculation on the transport dynamics of the Mississippi River, but images from the FlocARAZI confirm for the first time that suspended Mississippi River mud is indeed flocculated during both summer and winter.

3.2. The Vertical and Lateral Distributions of Floc d_{50}

The d_{50} by volume of the flocculated sediment is plotted over the depth for the BCS and VMC stations during summer and winter in Figure 4. During the summer survey, floc size data were collected at two lateral locations

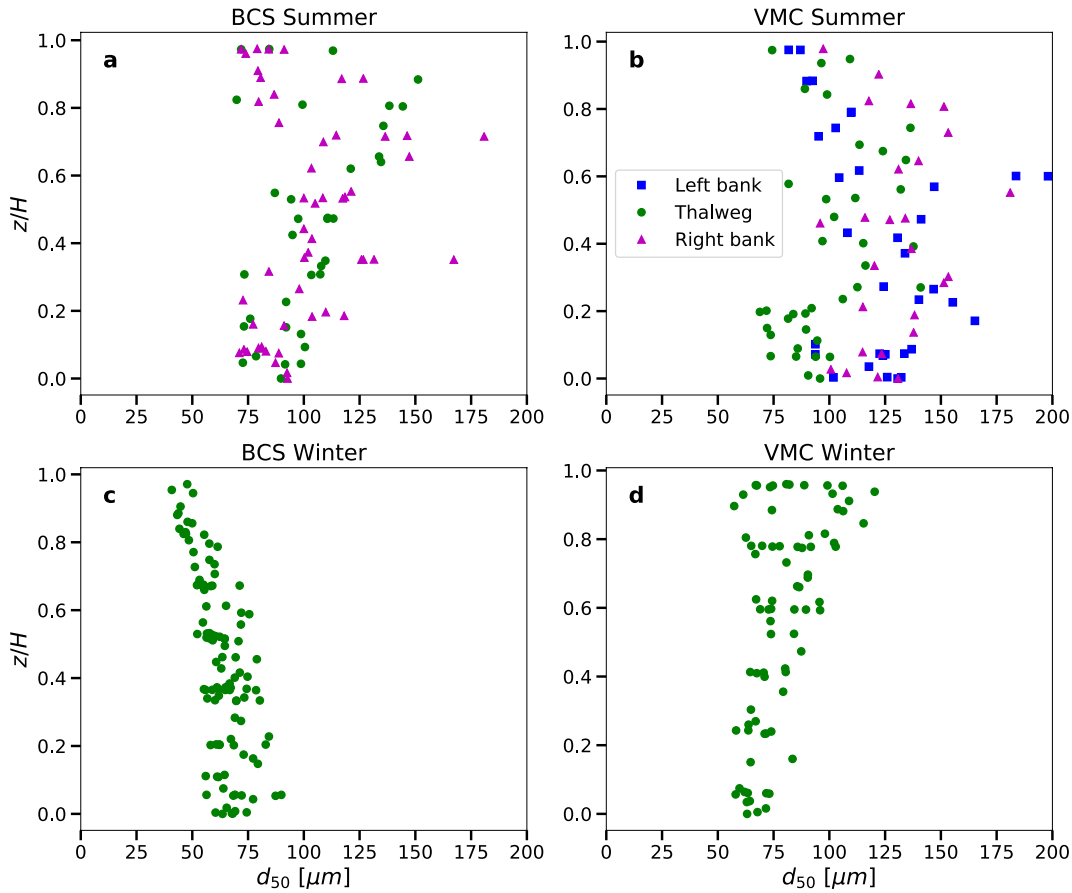

Figure 4. d_{50} floc size information collected at the Bonnet Carré Spillway (BCS) and Venice Main Channel locations during the summer and winter surveys. Floc size data were collected at multiple lateral locations during the summer survey, as indicated in panels (a, b). Floc size data were collected only in the thalweg during the winter survey (c, d). Though it appears that floc size increases with depth at the winter BCS station (c), this is a result of a large fraction of the observed particles consisting of silt and fine sand that could not be removed in the image processing. As such, the size information presented in panel (c) represents the d_{50} of flocs, coarse silts, and fine sands.

at the BCS station and three lateral locations at the VMC station; indicated in Figures 4a and 4b as being either the left bank, thalweg, or right bank. Floc size data were collected only at the thalweg location during the winter survey after observing little variation in size at different lateral stations across the section in the summer data.

No clear and consistent pattern in the d_{50} of the flocculated sediment with depth could be discerned. Measured d_{50} values did vary, and some trends with depth are present for some of the profiles, but no overall clear trend regarding the vertical distribution of d_{50} can be determined that could apply to all.

The floc d_{50} at the BCS during the summer ranged from approximately 75 to 100 μm near the bed, and 75–175 μm farther up in the water column (Figure 4a). A slight increase in floc size from the bed to around 75% of the flow depth is present, with a slight decrease in floc size near the water surface for the right bank station. Average floc d_{50} at the VMC location during the summer survey ranged from around 75 to around 135 μm near the bed (Figure 4b). Floc sizes from the surface to around 25% of the flow depth were relatively uniform, ranging from around 100 to 150 μm. The largest flocs were observed at the left and right-bank stations, where the largest d_{50} values were between 175 and 200 μm. d_{50} values at the VMC station during the winter ranged from around 60 μm near the bed to between 50 and 125 μm near the surface (Figure 4d). Floc sizes near the bed vary only slightly, between 55 and 75 μm, compared to farther up in the water column where both average d_{50} floc sizes increase and the range of sizes increases.

Though flocs were observed in suspension at the BCS during the winter survey, the data presented in Figure 4c represents the d_{50} sizes of flocs, silts, and fine sands. This is a result of the turbid conditions and images collected

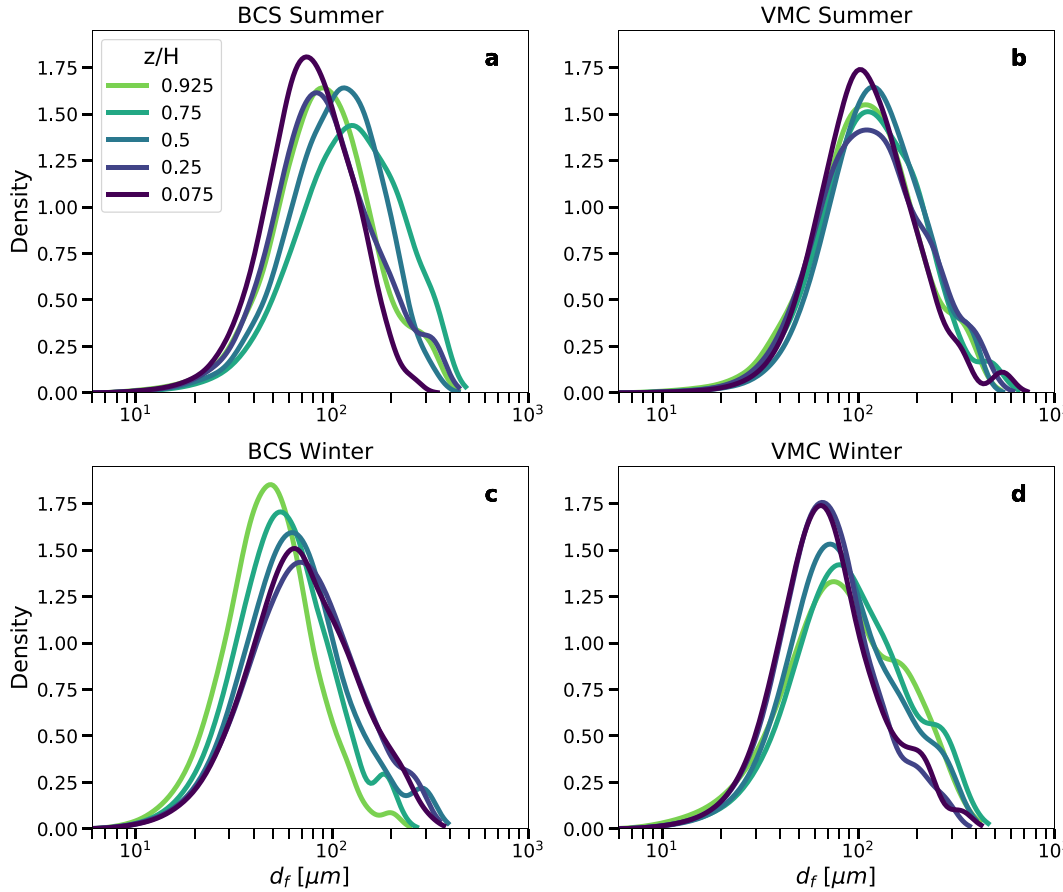

Figure 5. Kernel density estimates of the probability density function for floc size population data collected over specified ranges within the flow depth. Here z is taken as the vertical distance from the bed and H is the flow depth.

with the FlocARAZI containing a large amount of silt and sand. The algorithm used for identifying sand from image data was unable to identify sand correctly when flocs or silts overlapped with sand within the images. Medium to large sand was manually removed from the data, but a large number of very-fine sand grains within the data made it unfeasible to manually remove them from the data set. Therefore, the data presented in Figure 4c should not be taken to represent only flocs at the winter BCS location.

3.3. Floc Populations and Their Variation With Depth

A range of floc sizes were observed at all locations and depths. The previous section showed how the d_{50} of the size population varied over the depth at different stations and seasons. In this section, we show the distributions. The distributions are visualized as kernel density estimates (KDE) (Figure 5) and volume percent of flocs in a specified size range (Figure 6) at 7.5%, 25%, 50%, 75%, and 92.5% of the flow depth.

Two general statements regarding the distribution of flocs sizes can be made. The first is that all distributions contained one dominant peak in size (Figure 5). The second is that clustering of flocs within larger size classes was found to be present for flocs greater than approximately 100 µm. This clustering can be seen in the right-side tails of the KDE plots as a change in slope (Figure 5). No clear number of, or locations for, the inflection points applicable to all distributions is evident.

In all cases flocs in the 50–100 µm size range made up the bulk of the flocculated material by volume, that is, ≈40% (Figure 6) with the 100–150 µm range making up ≈20%–30%. This means that about 60%–70% of the flocculated mud, by volume, is between 50 and 150 µm in size. The largest flocs (>150 µm) compose 20%–30% on average, with the smallest flocs (<50 µm) 10%–20% on average (though this percentage for the smallest size class was higher for the VMC during winter).

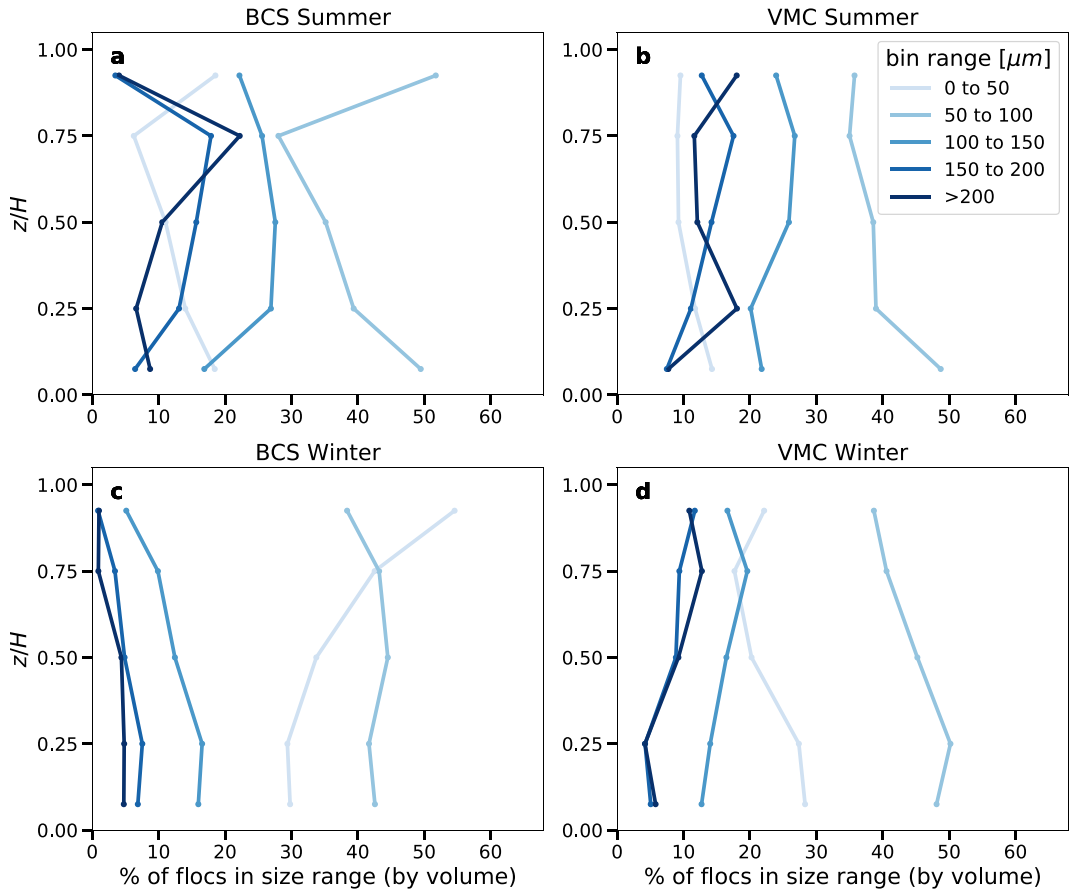

Figure 6. Floc size binned by volume into different size ranges at 7.5%, 25%, 50%, 75%, and 92.5% of the flow depth. Here z is taken as the vertical distance from the bed and H is the flow depth.

Changes in the distribution of these size fractions over the depth were relatively minor except when closest to the bed ($z/H = 0.075$) during summer. For both BCS and VMC, the binned data show a general decrease in the fraction of large flocs closest to the bed (Figures 6a and 6b). This decrease in the fraction of flocs in the larger size classes (>150 μm) was then accompanied by an increase in flocs within the smaller size classes. Another trend evident is that the percentage by volume of the largest flocs tended to increase slightly moving from the bed toward the free surface for both the BCS and VMS during summer and the VMC during winter. The one exception to this was the topmost point at BCS during summer (Figure 6).

The BCS winter KDE and volume percent of binned particles plots show a coarsening of suspended sediment from the surface to the bed (Figures 5c and 6c). Again, this is a result of the data for this particular station representing flocs, silt, and very-fine sand as previously noted.

3.4. Depth-Averaged Trends in Size by Station and Season

Depth-average values for the size statistics d_{16}, d_{50}, and d_{84} were calculated to allow for comparison of the average floc properties at different river stations in the same season and different seasons at the same station. During the same season, there was a small but noticeable change in the average size of the flocs moving down the river from the BCS to the VMC. On average, flocs at the VMC were larger than those at the BCS regardless of the season. For a given season, d_{50} increased by 10–15 μm going from the BCS to the VMC stations with d_{84} increasing by 30–40 μm (Table 3). This spatial change is possibly related to the overall decrease in river velocity and stress from the BCS down to VMC (Table 2).

A difference in the depth-averaged size of the flocs between seasons was observed at each station, and the magnitude of the seasonal difference was greater than that between stations during the same season. At both stations,

Table 3
Average Floc Sizes for Main Channel Stations

Station	d_{16} (μm)	d_{50} (μm)	d_{84} (μm)
BCS Summer	57	102	185
VMC Summer	66	116	213
BCS Winter[a]	35	63	119
VMC Winter	44	79	160

[a]The Bonnet Carré Spillway winter station includes both flocs and fine sand.

the floc d_{50} was ≈40 μm larger during the summer survey, with the d_{84} being ≈60 μm larger during the summer (Table 3). The 40 μm difference at the BCS was evident even though the winter size estimates were biased larger due to the presence of solid particles that could not be removed during image processing as previously discussed. The difference in floc sizes were also evident in the sample images from each station and survey (Figure 3).

3.5. Floc Settling Velocity and Mud Concentration Profiles

A Rouse profile was fit to the mud fraction of suspended sediment using SSC profiles collected at the BCS and VMC during both the summer and winter surveys. In addition, SWP1 from the winter survey is included in the analysis. Measured and calculated input parameters used for the analysis are presented in Table 2. In Table 2, values for the skin friction component of shear velocity were excluded for VMC and SWP1 during the winter survey since the bed consisted mainly of mud, and no bedforms were observed during the survey. The fit results are shown in Figure 7.

During the summer survey, settling velocities from the fit were 0.41 at the BCS and 0.52 mm/s at the VMC location (Figures 7a and 7b). This increase is consistent with the increase in floc size moving from the BCS to the VMC stations. Back-calculated floc density associated with these Rouse-profile derived settling velocities and the depth-averaged floc sizes at each station were ≈1,400 kg/m^3, if calculated using the model coefficients of $b_1 = 100$ and $b_2 = 0$, in Equation 12; using Stokes, that is, $b_1 = 18$ and $b_2 = 0$ puts floc density associated with this size and settling velocity at ≈1,070 kg/m^3.

During winter, effective settling velocity estimates from the fit were smaller for the BCS station relative to summer ($w_s = 0.07$ mm/s) due to the near well-mixed conditions that existed for $C = C(z)$ (Figure 7c). However, larger vertical concentration gradients of mud were observed downriver at VMC and SWP (Figures 7d and 7e). For these two locations during winter, the effective settling velocities obtained from the fit were 2.3 and 2.9 mm/s.

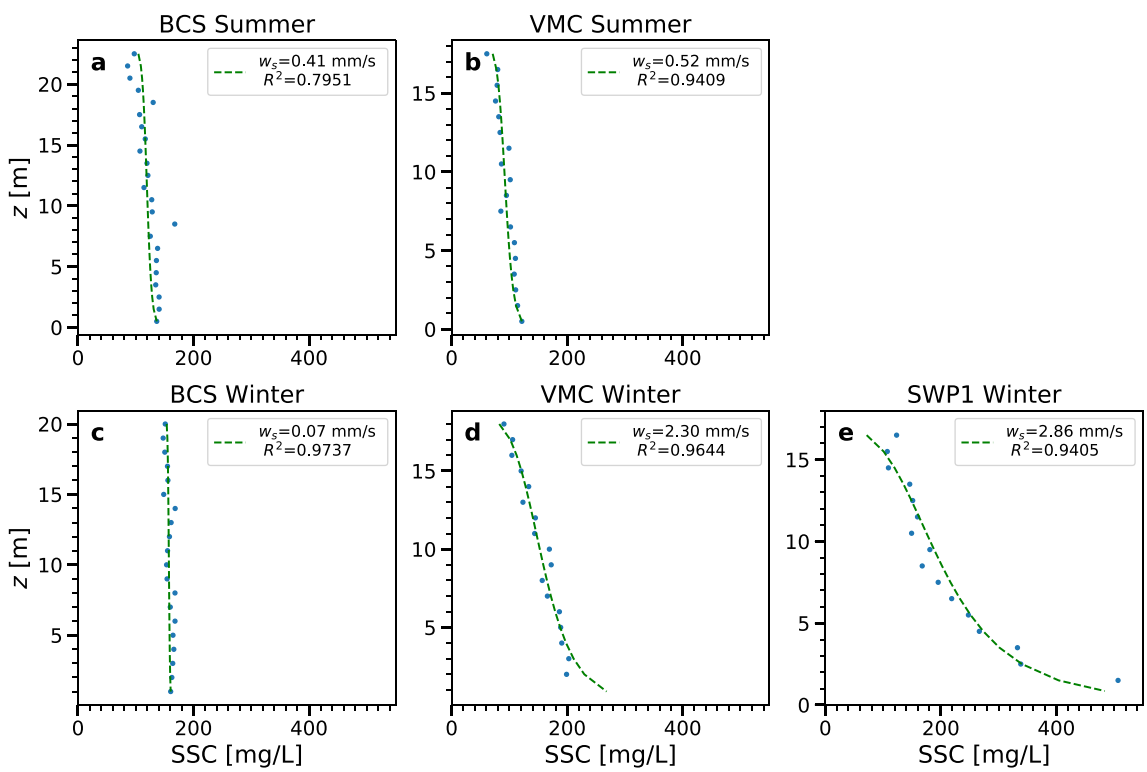

Figure 7. Mud fraction of suspended sediment concentration and fit Rouse profiles used to obtain an estimated bulk settling velocity.

Table 4
Settling Velocities Estimated From the Rouse Profile Analysis Compared to Calculations Based on Measured Floc Sizes and the Settling-Velocity Equation (Equation 12)

	w_s (mm/s)		n_f
Station	Rouse fit	Size-based calculations[a]	Fit based on sand coef.[b]
BCS Summer	0.4	0.5	1.90
VMC Summer	0.5	0.6	1.95
BCS Winter	0.1	0.2	1.50
VMC Winter	2.3	0.3	2.70
SWP1 Winter	2.9	0.3	2.70

[a]Calculations performed using the viscous floc settling coefficients of $b_1 = 100$, $b_2 = 0$, and $n_f = 2.5$. [b]Fractal dimensions, n_f, needed to make the calculated settling velocity, based on the nominal sand diameter coefficients of $b_1 = 20$ and $b_2 = 0.91$, match the settling velocity obtained from the Rouse profile fit.

Possible explanations for these high settling velocity estimates, relative to the other stations, are considered in the Discussion.

Settling velocity was also calculated using the measured floc sizes and Equation 12. The following input values were used to make the calculations: ν and ρ were adjusted for water temperature during the summer and winter; the primary particle size, d_p, was taken as 6 μm based on measurements of disaggregated samples; the density of the primary particles was taken to be $\rho_s = 2{,}650$ kg/m^3. Two sets of values for the coefficients b_1 and b_2 and the fractal dimension, n_f, were used. As a first pass, we used the viscous settling values of $b_1 = 100$, $b_2 = 0$, and $n_f = 2.5$ as suggested by Strom and Keyvani (2011) based on their fitting of historic floc settling data to estimate w_s based on the measured floc sizes. For the second set of coefficients, we used the standard values of $b_1 = 20$ and $b_2 = 0.91$ as suggested by Ferguson and Church (2004) based on the settling of solid sand using nominal, rather than sieved, particle size. We then varied the fractal dimension (equivalent with varying floc density) until the calculated value based on floc size matched the value obtained from the Rouse profile fit. In all cases, a bulk, volume-weighted settling velocity for the n number of flocs, with a volume, $V_{f,i}$, was calculated as: $w_s = \sum_{i=1}^{n} w_{s,i} V_{f,i} / \sum_{i=1}^{n} V_{f,i}$. The bulk settling velocity was calculated for the full set of flocs observed at a particular station.

For the BCS and VMC summer stations, the Strom and Keyvani (2011) settling velocity model coefficients and fractal dimension recommendations ($n_f = 2.5$, $b_1 = 100$, and $b_2 = 0$) produced average settling velocity values that matched well those from the Rouse profile analysis (Table 4). During the winter survey, the size measurements coupled with the recommended floc model coefficients produced settling velocity estimates that reasonably matched the Rouse profile fit values at the BCS station. However, the calculated values were an order of magnitude smaller than the Rouse estimates during winter at the VMC and SWP1 stations.

No match could be found between the profile estimates and size-based estimates of settling velocity during winter at VMC and SWP1 when using the viscous coefficients of $b_1 = 100$ and $b_2 = 0$ for any fractal dimension ≤ 3. To obtain a match for these two stations, we used the Ferguson and Church (2004) recommended solid sand coefficients of $b_1 = 20$ and $b_2 = 0.91$ and varied n_f until the w_s matched that from the Rouse fit. The same calculation was also performed on all other stations, and the output of the calculation is given in the last column of Table 4. In summary, the fractal dimension needed for summer was $n_f \approx 1.9$ and for winter $n_f \approx 2.7$.

4. Discussion

4.1. Spatial Distributions of Floc Sizes and the Role of Turbulence and Concentration in Setting Floc Size

Our study confirms that flocs were present within the freshwater reaches of the Mississippi River during both the summer and winter. To the best of our knowledge, this study presents the first direct in situ observations of flocs within the Mississippi River. Galler and Allison (2008) investigated the possibility of mud flocculation within the lower Mississippi River by collecting water samples with Niskin bottles to perform settling column tests on board their research vessel during a survey in June 2003. The observed settling rates led Galler and Allison (2008) to estimate that a third of the sediment mass within the settling column consisted of flocs smaller than 110 μm, and another third of the mass consisted of flocs larger than 567 μm. This range of floc sizes is in the range of floc sizes directly observed in this study during the summer survey. Similar mean floc sizes, in the range of 43–181 μm were observed with a LISST-100x at 23 stations along 1,532 km of the Yangtze River by L. Guo and He (2011).

We could not detect any consistent and persistent patterns in the distribution of floc sizes either laterally across the river channel or vertically over the depth. For this reason, as a first approximation, we suggest that floc sizes at a given river station can be assumed to be uniformly distributed over the cross-section. During some of the samplings, we did observe a clear trend of higher numbers of larger flocs near the free surface and higher numbers of smaller flocs near the boundary, a trend that has also been observed in some estuaries using a LISST-100x (e.g., Huang et al., 2022); though, the trend is not consistent in all estuaries and often depends on the position in the tide cycle (e.g., C. Guo et al., 2017; Uncles et al., 2010). This type of distribution in size over the depth

Table 5
Water Quality Measurements at USGS Gage Station 07374525 Mississippi River at Belle Chasse, LA Over Dates Closest to the Survey Study Date

Parameter	Summer	Winter
Date	23 June 2020	12 January 2021
T (°C)	27.4	6.9
SC (µS/cm)	362	348
pH	7.4	7.9
DO (mg/L)	5.9	12.1
N (mg/L)	2.3	1.7
P (mg/L)	0.18	0.32
DOC (mg/L)	3.4	2.95
Ca (mg/L)	40.6	30.9
Mg (mg/L)	14	10.3
Na (mg/L)	14	21.4
K (mg/L)	3.19	2.76
Cl (mg/L)	15.8	28.6
Fe (µg/L)	15.5	460

Note. The Belle Chasse station is located between the Bonnet Carré Spillway and Venice Main Channel sampling locations.

is perhaps explained by the increase in turbulent production and dissipation rate of turbulent kinetic energy near the boundary and the known inverse relationship between floc size and dissipation rate (Kuprenas et al., 2018; Tambo & Hozumi, 1979; van Leussen, 1994; Verney et al., 2009). Nevertheless, the pattern of larger flocs near the free surface and smaller flocs near the bed was not always observed. In addition, larger flocs were not correlated with the higher concentrations of mud found near the boundary. At all stations, mud concentration increased with depth regardless of river station or season (though the strength of the stratification with depth and station did vary). However, such increases in concentration with depth were not correlated with increased floc size. We, therefore, expect that floc sizes can respond to the overall average concentration in the river, but were less influenced by local depth-dependent variations in concentration; at least over the range of conditions we observed.

Floc sizes did respond, as expected, to changes in overall average shear. The Mississippi River at the BCS is narrower and more energetic than farther down the river at the VMC station. Velocities and shear velocity measurements are reflective of this with higher values at BCS relative to the VMC and water-column and image samples both reveal more sand in suspension at the BCS relative to the VMC station. Overall average concentration between the two sites was nearly equal with concentrations at the BCS being slightly larger. Floc sizes however were larger at the VMC during both seasons, indicating the floc size is dependent on the shear rate in the river but not on small changes in concentration.

4.2. Seasonal Effects on Floc Size

The differences in floc sizes over the depth, or from station to station, were all smaller than the differences in floc sizes observed from the summer to winter surveys at each individual station. Both summer and winter surveys took place during relatively high flow conditions at similar discharges, though the summer survey was made on the falling limb of a flow event and the winter survey was made on the rising limb. Average velocities and shear stresses were similar at each station from season to season. And turbidity measurements and calculated average suspended sediment values were also similar between the two surveys; though C_{avg} was slightly higher, on average, during the winter (Table 1).

While the flow rate, shear stress, and SSC were similar from survey to survey, differences in floc sizes between summer and winter were observed. Flocs were larger during summer than they were during winter. The d_{50} of the floc size distribution was approximately 40 µm larger in summer than in winter. The size difference in flocs between summer and winter could not have been due to differences in SSC since concentration was slightly larger during the winter. We also don't expect the size difference to be an outcome of changes in viscosity and hence the Kolmogorov micro-length scale. The lower water temperature in winter should have led to larger micro-length scales given the same overall average shear velocity and hence larger flocs in winter if the size difference were driven by turbulence conditions in the water column. Therefore we do not expect that the differences in floc sizes were driven by physical changes in turbulence or SSC. Instead, we expect that the difference in size was driven by differences in the chemistry (ion composition and concentration) or biology (organic material type and quantity) of the suspensions.

Water quality measurements made by the USGS at the Belle Chasse gage station 07374525, located between the BCS and VMC, over dates closest to our surveys are listed in Table 5. Specific conductance and ion composition and concentration were fairly consistent between the summer and winter, though specific conductance and the calcium and magnesium levels were all slightly higher during summer relative to winter (Tables 2 and 5). Abolfazli and Strom (2022) have shown that the presence of calcium chloride and magnesium chloride both can have a stronger influence on the flocculation potential of a suspension of natural mud than sodium chloride, and data from the Belle Chasse station do indicate that these ions were present at a slightly higher concentration during summer. However, the overall specific conductance values, while larger than those of headwater

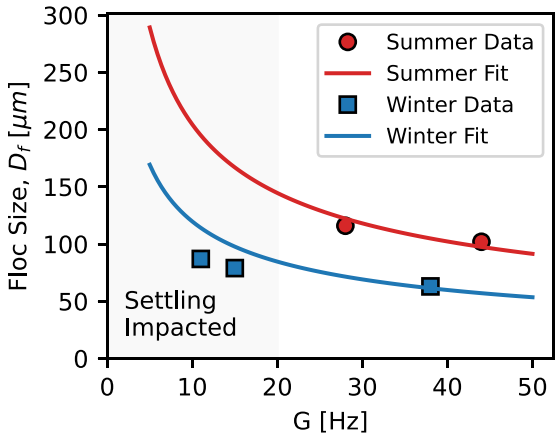

Figure 8. A model for equilibrium floc size as a function of concentration and shear rate, $d_{fe} = d_{fe}(C, G)$, fit to the summer and winter depth-averaged floc sizes at different river stations.

creeks (0–100 μS/cm), are still much less than what would be needed to produce 1 PSU, and it is unclear if the variation between summer and winter in terms of specific conductance (Table 2) is sufficient to account for the 40 μm change in the floc d_{50}. We suspect that it is not and that the difference in floc size between summer and winter is likely not driven by differences in ion concentration or type. pH is also known to influence flocculation rates and equilibrium size (Mietta et al., 2009), but the pH of the river varied little between our summer and winter surveys (Table 5).

The largest detectable difference from summer to winter in both our measurements and the water quality measures at the Belle Chasse station was that of water temperature (27°C during summer and 6°C during winter). Some water-treatment-focused studies have shown that temperature can change the optimum pH for flocculation at particular doses of some coagulants (Camp et al., 1940; Mohtadi & Rao, 1973), and in some cases, floc size (Fitzpatrick et al., 2004). However, there is little evidence that temperature alone can change the flocculation behavior of natural mud (Mohtadi & Rao, 1973). Therefore we do not expect that temperature itself was directly responsible for the difference in size observed between the seasons.

Taking all of the above into consideration, we suspect that a temperature-driven difference, or temperature co-varying difference, in a type of organic matter is likely the leading cause of the observed difference in floc sizes between summer and winter. Organic matter comes in many different forms. The most common measurement of organic content is that of Dissolved Organic Carbon (DOC). Yet, DOC does not vary markedly with season or discharge in the Mississippi River (e.g., Table 5), though it can be slightly higher during warmer temperatures and higher discharges (Cai et al., 2015). Furthermore, DOC concentration increases that are observed during high flows might primarily be sourced from organic constituents associated with terrestrial runoff that may or may not contribute to floc formation (Lee et al., 2019). What is known to enhance flocculation is EPS. EPS is known to be positively associated with Chlorophyll-a (Uncles et al., 2010) through algal production (Lee et al., 2019; Verney et al., 2009), and particle-attached bacterial communities. In the Mississippi River and elsewhere, increases in Chlorophyll-a are associated with warmer water temperatures and low-flow periods where mixing and sediment concentration are lower (Duan & Bianchi, 2006; Lee et al., 2019; Turner et al., 2022). Discharge conditions during the summer survey were not particularly low (Table 1) with respect to typical discharges associated with high Chlorophyll-a values (<15,000 m^3/s) (Turner et al., 2022).

Bacterial production, and specifically particle-associated bacterial production, is known to be strongly dependent on temperature in the Mississippi River regardless of flow discharge (Ochs et al., 2010; Payne et al., 2020). Therefore, we suspect that the increase in observed floc sizes in the summer was primarily due to the increased activity of particle-attached bacterial secreting EPS and enhancing the capture potential and strength of the mud aggregates. Similar correlations between water temperature and floc size and strength have been made by Droppo et al. (1998) and Egan et al. (2022), both of whom suggest that increasing temperature leads to an increase in the productivity of the particle-attached bacteria and associated enhancement of EPS. Therefore, while tightly controlled data linking floc size to increased bacterial production brought on by temperature changes is not available in our study or the studies of Droppo et al. (1998) and Egan et al. (2022), all three point to the utility of temperature as a proxy for EPS production and hence floc aggregation efficiency and strength. For example, calibration of the equilibrium floc size model (see Appendix A for details), which yields $d_{fe} = d_{fe}(C, G)$, of Winterwerp (1998) can be made for summer and winter along the Mississippi at the different stations by increasing the ratio of the aggregation to breakup efficiency terms, k'_A/k'_B, by a factor of 5 (Figure 8). It is conceivable then, that given enough data, one could develop a relationship for $k'_A/k'_B = k'_A/k'_B(T)$.

4.3. Can Floc Size Explain Vertical Gradients in Mud Concentration?

Flocculation has the potential to increase the settling velocity of mud relative to that predicted by disaggregated particle sizes. For example, the calculated settling velocities for the summer survey at the BCS and VMC range from 0.41 to 0.53 mm/s. These settling velocities correspond to an equivalent silt grain with a diameter between 25 and 30 μm. However, considering that the characteristic primary particle size that makes up the flocs is likely

between 5 and 10 μm, the calculated floc settling velocities are approximately an order of magnitude higher than the settling velocity of the characteristic primary particles.

If mud within a river is unflocculated, the unaggregated particles would be expected to be distributed uniformly over the water column as a result of their small settling velocities. However, it is possible that the presence of flocs, and hence increased settling velocity of the mud, could result in vertical concentration gradients of mud in rivers. Recently Lamb et al. (2020) analyzed disaggregated mud size and concentration profile data obtained from a range of field measurements. They hypothesized that if flocculation of mud was present, this could be observed through vertical variations in mud concentration of individual grain-size classes. That is, vertical variations in concentration would be present for size classes that would be expected to be distributed uniformly over the water column if no flocculation was present. They tested this hypothesis by analyzing individual grain-size classes from the mud size and concentration data, from the multiple data sources, in a Rouse profile analysis to obtain effective settling velocities for each grain-size class. Their results indicated that effective-settling velocities for mud range from 0.17 to 0.70 mm/s, with a geometric mean of 0.34 mm/s. This range of settling rates is in agreement with the 0.2–0.6 mm/s settling velocity of mud calculated in this study from direct observations of mud floc sizes in the lowermost Mississippi River during the summer and winter.

The settling velocities calculated from observed sizes matched well those calculated from the Rouse profile analysis for all summer survey locations and the BCS during winter using the Strom and Keyvani (2011) recommended settling velocity model coefficients of $b_1 = 100$, $b_2 = 0$, and $n_f = 2.5$ without any model tuning (Table 4 middle column) Therefore we conclude that flocculated mud was the primary driver of the observed concentration gradients during summer. However, Rouse profile w_s values during winter at VMC and SWP1 (the two sites with mud beds) exceeded those of summer and values estimated from the floc size distributions for winter using the recommended model coefficients. Possible explanations for the mismatch include: (a) the assumption that form drag is insignificant is incorrect and should be accounted for in the shear velocity calculation for the two sites with mud beds; (b) the possibility that more free or floc-bound solid silica silt was present in winter relative to summer; and/or (c) the mud beds observed at VMC and SWP1 during the winter were net erosional as river discharge increased over the course of the survey, violating the Rouse profile assumption that erosion of the bed is in equilibrium with deposition and thereby resulting in higher near-bed concentrations than would be expected under equilibrium conditions.

The assumption that the form drag component of shear velocity was negligible during the winter survey at VMC and SWP1 was made as a result of not observing large-scale bedform contours from single-beam sonar images observed while onboard the research vessel. If the skin friction component of shear velocity at VMC and SWP1 during the winter was calculated with Equation 9, the values associated with the stations would decrease to 0.023 and 0.018 m/s. Applying this decrease in shear velocity to the Rouse profile analysis reduces the estimated settling velocities to 1.07 and 1.32 mm/s for VMC and SWP1 during the winter survey—a nearly 54% decrease at both stations. However, even if form stress was removed, w_s from the Rouse profile fit would still be substantially larger than those calculated from imaged particle sizes with $n_f = 2.5$ and coefficients $b_1 = 100$ and $b_2 = 0$.

During the winter survey, water-column samples were filtered directly for concentration without sizing of the particles. Therefore, it is possible that a larger amount of free or floc-bound silica silt was present in the samples, thereby resulting in an overall larger suspension-average particle or floc density and higher settling velocities. From visual inspection of the images, we conclude that both free and floc-bound solid silt is present in suspension at all sampling locations during both summer and winter. Qualitatively, it did appear that there might have been a larger volume of solid silt in the winter samples at VMC relative to that of summer. If true, the increase in silt content could lead to increases in the settling velocity of a floc of a given size due to the incorporation of solid particles within flocs, thereby increasing the average floc density. Such behavior has been observed in mixtures of mud and suspended sand (Manning et al., 2010, 2011; Spearman et al., 2011) and silt (Tran & Strom, 2017). However, we were not able to quantify rigorously the amount of free or floc-bound silt from the images. Therefore the visual-inspection observation remains speculative and in need of other forms of quantitative assessment.

Another possible explanation for the higher estimated Rouse-profile w_s at VMC and SWP1 during winter could be that the freshly exposed mud bed was net erosional. An assumption in the development of the Rouse profile is that bed erosion and deposition are in equilibrium. If the bed were net erosional, then this assumption would be violated and could potentially lead to concentrations near the bed that are higher than what would be present during equilibrium conditions. It was hypothesized that the mud bed at VMC and SWP1 observed during the

winter survey was deposited in the presence of a salt wedge that had migrated upriver past these stations as a result of low river discharge proceeding the survey. When a salt wedge is in place, the major shear interface moves from the bed to the contact point between the fresh and salt water. In such conditions, ephemeral mud layers are known to develop in coastal, microtidal rivers (Carlin et al., 2015; Galler & Allison, 2008). In the week leading up to the survey, river discharge in the Mississippi had increased substantially and pushed the salt wedge out of the main channel, and exposed the fresh mud deposits to shear from the river flow. During the survey period, we measured the downstream retreat of the salt wedge in SWP. Grab samples of the bed at the VMC and SWP1 stations during winter yielded homogeneous mud. While no erosional tests were performed on the mud, we expect that the flow conditions at the time (u_* on the order of 0.05 m/s and $\tau_B = \rho u_*^2 \approx 2.5$ Pa) could produce a net erosional bed. Mud beds often begin to erode at bed shear stresses less than 1 Pa (Grabowski et al., 2011; Van Prooijen & Winterwerp, 2010; Wiberg et al., 2013), and mud layers deposited under a salt wedge in the Mississippi and Brazos rivers are known to be ephemeral (Carlin et al., 2015; Galler & Allison, 2008) due to erosion and downstream export of the mud that takes place upon the expulsion of the salt wedge.

Can measured floc sizes, and their associated calculated settling velocities, explain the gradients in mud concentration observed over the vertical in the lower reaches of the Mississippi River? Our data suggest that they could for the summer surveys (i.e., Rouse profile-derived settling velocities matched expected values from floc size measurements and standard floc settling velocity values). However, the link between Rouse settling velocity and measured size was more nuanced for two of the stations for which a thick unconsolidated mud bed was present during winter. If we assume that the density of the suspended particles at these two sites was larger during winter than it was during summer and that the settling velocity of the particles and flocs are better characterized by typical sand settling coefficients (i.e., use of $n_f = 2.7$, $b_1 = 20$, and $b_2 = 0.91$ rather than $n_f = 2.5$, $b_1 = 100$, $b_2 = 0$), then yes, the measured sizes are able to explain the Rouse profile extracted settling velocity. Based on visual inspection of the images it appears possible that there was a larger degree of solid silt particles incorporated into the flocs at these two stations during the winter survey compared to the flocs during summer. The presence of additional solid silt relative to summer should lead to overall higher density and faster-settling flocs for a given size during winter. However, changes in the settling velocity model coefficients were not needed to explain the observed Rouse extracted settling velocity for the BCS station during winter (the upstream station with a sand bed), suggesting that the increase in Rouse profile extracted settling velocity might be related to the bed type more so than winter versus summer conditions. We speculate that at least part of the large increase in Rouse profile-derived settling velocity for the winter measurements at VMC and SWP1 was due to the presence of a net erosional bed. If this is true, it highlights the need to be cautious when extracting settling velocity values from the Rouse profile over actively eroding mud beds that may take longer to establish equilibrium than sand beds.

5. Conclusions

This study presents the first direct measurements of floc sizes within the lowermost freshwater reaches of the Mississippi River, from the BCS downstream to SWP. Measurements were made at different longitudinal, lateral, and vertical positions within the river channel during summer 2020 and winter 2021 at a river discharge of ≈19,000 m^3/s and average suspended sediment concentrations of ≈150 mg/l in both surveys. At all sampling locations, suspended mud flocs comprised of clay and silt were observed in both the winter and summer surveys. The exact proportion of the mud which exists in flocculated form is difficult to determine, but flocs were the dominant particulate form present in the images.

Overall, our study highlights that the majority of the mud (both silt and clay), in both summer and winter, in the lowermost freshwater reaches of the Mississippi River appears to be flocculated and that the floc size can be reasonably represented with a cross-sectional averaged value that is dependent on turbulent shear and season. Depth-averaged floc sizes increased slightly moving downriver as turbulence levels dropped, but floc sizes varied little over the flow depth or laterally across a cross-section. During the summer survey, mean floc sizes were observed to range from 75 to 200 μm. Whereas in the winter mean floc sizes ranged from 50 to 125 μm.

One question we sought to explore in this study was whether or not measured floc sizes could explain observed vertical gradients in mud concentration profiles. Data and analysis suggest that floc size appears to explain well vertical variations in mud concentration profiles when the bed was predominately composed of sand. Suspension average mud settling velocities for these cases ranged from 0.1 to 0.5 mm/s. However, at two of the winter stations where a mud bed existed, Rouse-profile estimated settling velocities ranged from 1 to 3 mm/s depending on the

analysis method. These values exceeded the size-based estimates of settling velocity unless the measured flocs were treated as being closer in density and shape to solid particles. The increase in the Rouse profile estimated settling velocity could have been the result of a larger fraction of free or floc-bound silt in suspension at those sites and/or the presence of an actively eroding mud bed that resulted in disequilibrium conditions between erosion and deposition.

These measurements show the importance of flocculation and its influence on mud settling rates in the Mississippi River upstream of marine saltwater influence. While we were not able to measure directly the fraction of mud that existed in floc form (since mud could have existed below the resolution of our camera system), the imaged suspensions in the 10 μm and larger range visually displayed a high degree of flocculation. The data point to the importance of the organic matter, river background ion composition, and turbulence as important drivers in setting the settling characteristics of the mud within the river. In addition, the presence of flocs in the freshwater reaches of the river has bearing on how fast mud settles once passing through natural or man-made openings in river banks and into surrounding brackish embayments. The boundary condition for mud size and settling velocity in such cases should correspond with a flocculated state. The addition of salt or decrease in turbulence outside of the main channel could potentially still increase the size and settling velocity, but we surmise that very little time or distance is needed to reach a new equilibrium since that starting condition is already flocculated. Based on spot measures elsewhere in the Mississippi River basin, we expect that the findings present here are not unique to the Mississippi River. However, additional in situ observations are needed both with the Mississippi and elsewhere to understand fully the role of the hydrodynamic, suspended sediment quantity and composition, organic material, and ions in controlling floc size and settling velocities within the fluvial environment more generally.

Appendix A: Equilibrium Floc Size Model Fit

The equilibrium floc size model of Winterwerp (1998) for $d_{fe} = d_{fe}(C, G)$ takes the following basic form:

$$d_{50} = d_p + \frac{k_A C}{k_B \sqrt{G}} \tag{A1}$$

where d_p is the disaggregated primary or constituent particle size, C is the mass concentration of sediment, and k_A and k_B are the aggregation and breakup coefficients defined as:

$$k_A = \frac{k'_A}{n_f} \frac{d_p^{n_f - 3}}{\rho_s} \tag{A2}$$

and,

$$k_B = \frac{k'_B}{n_f} d_p^{-p} \left(\frac{\mu}{F_y} \right)^q \tag{A3}$$

In Equations A2 and A3, n_f is the fractal dimension of the flocs, ρ_s density of the dry unflocculated sediment, μ is the dynamic viscosity of the water, F_y is the yield strength of the flocs, k'_A and k'_B are aggregation and breakup efficiency coefficients, and p and q are model parameters. Through a scaling argument, p is typically taken to be $p = 3 - n_f$ (Kuprenas et al., 2018; Winterwerp, 1998). And following the reasoning of Kuprenas et al. (2018) and set q to be a simple function of the size of the flocs relative to the Kolmogorov microscale, $\eta = \sqrt{G/\nu}$:

$$q = c_1 + c_2 \frac{d_{50}}{\eta} \tag{A4}$$

where c_1 and c_2 are constant coefficients. The proposed formulation ensures k_B increases as d_{50} approaches η.

For the fit to the Mississippi River data, we used the profile averaged measurements of d_50, concentration, and G; depth-averaged G was estimated from the data using $G = \sqrt{U u_*^2/(\nu H)}$. Water density and viscosity were set based on water temperature and salinity of zero. Other model coefficients used included: $d_p = 6$ μm, $\rho_s = 2{,}650$ kg/m^3, $F_y = 10^{-10}$ N, $c_1 = 0.5$, $c_2 = 1.5$, and $n_f = 2$. Reasonable values for k'_A/k'_B needed to describe the data under these conditions were $k'_A/k'_B = 1.5 \times 10^5$ during summer and $k'_A/k'_B = 3.0 \times 10^4$ during winter. These ratios are used to produce the fit lines of Figure 8.

Data Availability Statement

Raw data that support the findings of this study are publicly available online at https://github.com/FlocData/Data-Osborn-et-al-Mississippi (Strom et al., 2023).

Acknowledgments
Funding for this work was provided by the National Science Foundation under EAR award 1801142, "Collaborative Research: Flocculation Dynamics in the Fluvial to Marine Transition." Additional financial support for R.O. was provided by the Charles E. Via, Jr. Endowment at Virginia Tech and the New Horizons Graduate Scholars Program. We are also grateful to the USACE Bonnet Carré Spillway Office for operational support. Three anonymous reviewers and the editor Ton Hoitink provided helpful comments and critiques of the manuscript; we are grateful for their efforts.

References

Abolfazli, E., & Strom, K. (2022). *Deicing road salts may contribute to impairment of streambeds through alterations to sedimentation processes*. ACS ES&T Water.

Allison, M. A., Demas, C. R., Ebersole, B. A., Kleiss, B. A., Little, C. D., Meselhe, E. A., et al. (2012). A water and sediment budget for the lower Mississippi–Atchafalaya River in flood years 2008–2010: Implications for sediment discharge to the oceans and coastal restoration in Louisiana. *Journal of Hydrology*, *432–433*(0), 84–97. https://doi.org/10.1016/j.jhydrol.2012.02.020

Bungartz, H., Krüger, A., & Engelhardt, C. (2006). Fluvial suspended sediment dynamics: Implications for particulate organic carbon transport modeling. *Water Resources Research*, *42*(10), W10424. https://doi.org/10.1029/2005wr004486

Cai, Y., Guo, L., Wang, X., & Aiken, G. (2015). Abundance, stable isotopic composition, and export fluxes of DOC, POC, and DIC from the Lower Mississippi River during 2006–2008. *Journal of Geophysical Research: Biogeosciences*, *120*(11), 2273–2288. https://doi.org/10.1002/2015jg003139

Camp, T. R., Root, D. A., & Bhoota, B. V. (1940). Effects of temperature on rate of floc formation. *Journal (American Water Works Association)*, *32*(11), 1913–1927. https://doi.org/10.1002/j.1551-8833.1940.tb19608.x

Carlin, J. A., Dellapenna, T. M., Strom, K., & Noll, C. J. (2015). The influence of a salt wedge intrusion on fluvial suspended sediment and the implications for sediment transport to the adjacent coastal ocean: A study of the lower Brazos River TX, USA. *Marine Geology*, *359*, 134–147. https://doi.org/10.1016/j.margeo.2014.11.001

Cartwright, G. M., Friedrichs, C. T., & Sanford, L. P. (2011). In situ characterization of estuarine suspended sediment in the presence of muddy flocs and pellets. In P. Wang, J. D. Rosati, & T. M. Roberts (Eds.) (Vol. 1, pp. 642–654).*The proceedings of the coastal sediments*.

Deng, Z., He, Q., Chassagne, C., & Wang, Z. B. (2021). Seasonal variation of floc population influenced by the presence of algae in the Changjiang (Yangtze River) Estuary. *Marine Geology*, *440*, 106600. https://doi.org/10.1016/j.margeo.2021.106600

Droppo, I. G., Jeffries, D., Jaskot, C., & Backus, S. (1998). The prevalence of freshwater flocculation in cold regions: A case study from the Mackenzie River Delta, Northwest Territories, Canada. *Arctic*, *51*(2), 155–164. https://doi.org/10.14430/arctic1056

Droppo, I. G., Leppard, G. G., Flannigan, D. T., & Liss, S. N. (1997). The freshwater floc: A functional relationship of water and organic and inorganic floc constituents affecting suspended sediment properties. In *The Interactions Between Sediments and Water: Proceedings of the 7th International Symposium, Baveno* (Vol. 99, No. (1–4), pp. 43–53). https://doi.org/10.1007/bf02406843

Droppo, I. G., & Ongley, E. (1994). Flocculation of suspended sediment in rivers of southeastern Canada. *Water Research*, *28*(8), 1799–1809. https://doi.org/10.1016/0043-1354(94)90253-4

Duan, S., & Bianchi, T. S. (2006). Seasonal changes in the abundance and composition of plant pigments in particulate organic carbon in the lower Mississippi and Pearl Rivers. *Estuaries and Coasts*, *29*(3), 427–442. https://doi.org/10.1007/bf02784991

Egan, G., Chang, G., Manning, A. J., Monismith, S., & Fringer, O. (2022). On the variability of floc characteristics in a shallow estuary. *Journal of Geophysical Research: Oceans*, *127*(6), e2021JC018343. https://doi.org/10.1029/2021jc018343

Eisma, D. (1986). Flocculation and de-flocculation of suspended matter in estuaries. *Netherlands Journal of Sea Research*, *20*(2–3), 183–199. https://doi.org/10.1016/0077-7579(86)90041-4

Fall, K. A., Friedrichs, C. T., Massey, G. M., Bowers, D. G., & Smith, S. J. (2021). The importance of organic content to fractal floc properties in estuarine surface waters: Insights from video, LISST, and pump sampling. *Journal of Geophysical Research: Oceans*, *126*(1), e2020JC016787. https://doi.org/10.1029/2020jc016787

Fennessy, M. J., Dyer, K. R., & Huntley, D. A. (1994). INSSEV: An instrument to measure the size and settling velocity of flocs in situ. *Marine Geology*, *117*(1–4), 107–117. https://doi.org/10.1016/0025-3227(94)90009-4

Ferguson, R., & Church, M. (2004). A simple universal equation for grain settling velocity. *Journal of Sedimentary Research*, *74*(6), 933–937. https://doi.org/10.1306/051204740933

Fettweis, M., & Baeye, M. (2015). Seasonal variation in concentration, size, and settling velocity of muddy marine flocs in the benthic boundary layer. *Journal of Geophysical Research: Oceans*, *120*(8), 5648–5667. https://doi.org/10.1002/2014jc010644

Fettweis, M., Schartau, M., Desmit, X., Lee, B. J., Terseleer, N., Van der Zande, D., et al. (2022). Organic matter composition of biomineral flocs and its influence on suspended particulate matter dynamics along a nearshore to offshore transect. *Journal of Geophysical Research: Biogeosciences*, *127*(1), e2021JG006332. https://doi.org/10.1029/2021jg006332

Fitzpatrick, C., Fradin, E., & Gregory, J. (2004). Temperature effects on flocculation, using different coagulants. *Water Science and Technology*, *50*(12), 171–175. https://doi.org/10.2166/wst.2004.0710

Fox, J., Ford, W., Strom, K., Villarini, G., & Meehan, M. (2013). Benthic control upon the morphology of transported fine sediments in a low-gradient stream. *Hydrological Processes*, *28*(11), 3776–3788. https://doi.org/10.1002/hyp.9928

Galler, J. J., & Allison, M. A. (2008). Estuarine controls on fine-grained sediment storage in the Lower Mississippi and Atchafalaya Rivers. *Geological Society of America Bulletin*, *120*(3–4), 386–398. https://doi.org/10.1130/b26060.1

Gibbs, R. J. (1985). Estuarine flocs: Their size, settling velocity and density. *Journal of Geophysical Research*, *90*(C2), 3249–3251. https://doi.org/10.1029/jc090ic02p03249

Grabowski, R. C., Droppo, I. G., & Wharton, G. (2011). Erodibility of cohesive sediment: The importance of sediment properties. *Earth-Science Reviews*, *105*(3–4), 101–120. https://doi.org/10.1016/j.earscirev.2011.01.008

Guo, C., He, Q., Guo, L., & Winterwerp, J. C. (2017). A study of in-situ sediment flocculation in the turbidity maxima of the Yangtze Estuary. *Estuarine, Coastal and Shelf Science*, *191*, 1–9. https://doi.org/10.1016/j.ecss.2017.04.001

Guo, L., & He, Q. (2011). Freshwater flocculation of suspended sediments in the Yangtze River, China. *Ocean Dynamics*, *61*(2–3), 371–386. https://doi.org/10.1007/s10236-011-0391-x

Horemans, D. M. L., Dijkstra, Y. M., Schuttelaars, H. M., Sabbe, K., Vyverman, W., Meire, P., & Cox, T. J. S. (2021). Seasonal variations in flocculation and erosion affecting the large-scale suspended sediment distribution in the Scheldt estuary: The importance of biotic effects. *Journal of Geophysical Research: Oceans*, *126*(4), e2020JC016805. https://doi.org/10.1029/2020jc016805

Huang, J., Wang, S., Li, X., Xie, R., Sun, J., Shi, B., et al. (2022). Effects of shear stress and salinity stratification on floc size distribution during the dry season in the Modaomen Estuary of the Pearl River. *Frontiers in Marine Science*, *9*, 836927. https://doi.org/10.3389/fmars.2022.836927

Izquierdo-Ayala, K., Garcia-Aragon, J. A., Castillo-Uzcanga, M. M., & Salinas-Tapia, H. (2021). Freshwater flocculation dependence on turbulence properties in the Usumacinta River. *Journal of Hydraulic Engineering*, *147*(12), 05021009. https://doi.org/10.1061/(asce)hy.1943-7900.0001940

Keyvani, A., & Strom, K. (2013). A fully-automated image processing technique to improve measurement of suspended particles and flocs by removing out-of-focus objects. *Computers & Geosciences*, *52*, 189–198. https://doi.org/10.1016/j.cageo.2012.08.018

Kim, J.-W., & Nestmann, F. (2009). Settling behavior of fine-grained materials in flocs. *Journal of Hydraulic Research*, *47*(4), 492–502. https://doi.org/10.1080/00221686.2009.9522025

Kranck, K. (1973). Flocculation of suspended sediment in the sea. *Nature*, *246*(5432), 348–350. https://doi.org/10.1038/246348a0

Kranck, K. (1980). Experiments on the significance of flocculation in the settling of fine-grained sediment in still water. *Canadian Journal of Earth Sciences*, *17*(11), 1517–1526. https://doi.org/10.1139/e80-159

Kranck, K., & Milligan, T. G. (1992). Characteristics of suspended particles at an 11-hour anchor station in San Francisco Bay, California. *Journal of Geophysical Research*, *97*(C7), 11373–11382. https://doi.org/10.1029/92jc00950

Kranenburg, C. (1994). The fractal structure of cohesive sediment aggregates. *Estuarine, Coastal and Shelf Science*, *39*(5), 451–460. https://doi.org/10.1006/ecss.1994.1075

Kuprenas, R., Tran, D., & Strom, K. (2018). A shear-limited flocculation model for dynamically predicting average floc size. *Journal of Geophysical Research: Oceans*, *123*(9), 6736–6752. https://doi.org/10.1029/2018jc014154

Lamb, M. P., de Leeuw, J., Fischer, W. W., Moodie, A. J., Venditti, J. G., Nittrouer, J. A., et al. (2020). Mud in rivers transported as flocculated and suspended bed material. *Nature Geoscience*, *13*(8), 566–570. https://doi.org/10.1038/s41561-020-0602-5

Le, H.-A., Gratiot, N., Santini, W., Ribolzi, O., Tran, D., Meriaux, X., et al. (2020). Suspended sediment properties in the Lower Mekong River, from fluvial to estuarine environments. *Estuarine, Coastal and Shelf Science*, *233*, 106522. https://doi.org/10.1016/j.ecss.2019.106522

Lee, B. J., Hur, J., & Toorman, E. A. (2017). Seasonal variation in flocculation potential of river water: Roles of the organic matter pool. *Water*, *9*(5), w9050335. https://doi.org/10.3390/w9050335

Lee, B. J., Kim, J., Hur, J., Choi, I. H., Toorman, E. A., Fettweis, M., & Choi, J. W. (2019). Seasonal dynamics of organic matter composition and its effects on suspended sediment flocculation in river water. *Water Resources Research*, *55*(8), 6968–6985. https://doi.org/10.1029/2018wr024486

Lefebvre, J.-P., Ouillon, S., Vinh, V., Arfi, R., Panché, J.-Y., Mari, X., et al. (2012). Seasonal variability of cohesive sediment aggregation in the Bach Dang–Cam Estuary, Haiphong (Vietnam). *Geo-Marine Letters*, *32*(2), 103–121. https://doi.org/10.1007/s00367-011-0273-8

Liss, S. N., Droppo, I. G., Flannigan, D. T., & Leppard, G. G. (1996). Floc architecture in wastewater and natural riverine systems. *Environmental Science & Technology*, *30*(2), 680–686. https://doi.org/10.1021/es950426r

Manning, A. J., Baugh, J. V., Spearman, J. R., Pidduck, E. L., & Whitehouse, R. J. S. (2011). The settling dynamics of flocculating mud-sand mixtures: Part 1—Empirical algorithm development. *Ocean Dynamics*, *61*(2), 311–350. https://doi.org/10.1007/s10236-011-0394-7

Manning, A. J., Baugh, J. V., Spearman, J. R., & Whitehouse, R. J. S. (2010). Flocculation settling characteristics of mud: Sand mixtures. *Ocean Dynamics*, *60*(2), 237–253. https://doi.org/10.1007/s10236-009-0251-0

Manning, A. J., & Dyer, K. R. (2002a). A comparison of floc properties observed during neap and spring tidal conditions. In J. C. Winterwerp & C. Kranenburg (Eds.), *Fine sediment dynamics in the marine environment* (Vol. 5, pp. 233–250). Elsevier.

Manning, A. J., & Dyer, K. R. (2002b). The use of optics for the in situ determination of flocculated mud characteristics. *Journal of Optics A: Pure and Applied Optics*, *4*(4), S71–S81. https://doi.org/10.1088/1464-4258/4/4/366

Markussen, T. N., & Andersen, T. J. (2013). A simple method for calculating in situ floc settling velocities based on effective density functions. *Marine Geology*, *344*, 10–18. https://doi.org/10.1016/j.margeo.2013.07.002

Markussen, T. N., Elberling, B., Winter, C., & Andersen, T. J. (2016). Flocculated meltwater particles control Arctic land-sea fluxes of labile iron. *Scientific Reports*, *6*(1), 24033. https://doi.org/10.1038/srep24033

Marttila, H., & Kløve, B. (2015). Spatial and temporal variation in particle size and particulate organic matter content in suspended particulate matter from peatland-dominated catchments in Finland. *Hydrological Processes*, *29*(6), 1069–1079. https://doi.org/10.1002/hyp.10221

Mehta, A. J. (2022). *An introduction to hydraulics of fine sediment transport* (Vol. 56). World Scientific.

Mietta, F., Chassagne, C., Manning, A. J., & Winterwerp, J. (2009). Influence of shear rate, organic matter content, pH and salinity on mud flocculation. *Ocean Dynamics*, *59*(5), 751–763. https://doi.org/10.1007/s10236-009-0231-4

Mikkelsen, O. A., Hill, P. S., & Milligan, T. G. (2007). Seasonal and spatial variation of floc size, settling velocity, and density on the inner Adriatic Shelf (Italy). *Continental Shelf Research*, *27*(3–4), 417–430. https://doi.org/10.1016/j.csr.2006.11.004

Mikkelsen, O. A., Hill, P. S., Milligan, T. G., & Chant, R. J. (2005). In situ particle size distributions and volume concentrations from a LISST-100 laser particle sizer and a digital floc camera. *Continental Shelf Research*, *25*(16), 1959–1978. https://doi.org/10.1016/j.csr.2005.07.001

Mohtadi, M. F., & Rao, P. N. (1973). Effect of temperature on flocculation of aqueous dispersions. *Water Research*, *7*(5), 747–767. https://doi.org/10.1016/0043-1354(73)90091-2

Nghiem, J. A., Fischer, W. W., Li, G. K., & Lamb, M. P. (2022). A mechanistic model for mud flocculation in freshwater rivers. *Journal of Geophysical Research: Earth Surface*, *127*(5), e2021JF006392. https://doi.org/10.1029/2021jf006392

Nittrouer, J. A., Mohrig, D., & Allison, M. (2011). Punctuated sand transport in the lowermost Mississippi River. *Journal of Geophysical Research*, *116*(F4), F04025. https://doi.org/10.1029/2011jf002026

Ochs, C. A., Capello, H. E., & Pongruktham, O. (2010). Bacterial production in the lower Mississippi River: Importance of suspended sediment and phytoplankton biomass. *Hydrobiologia*, *637*(1), 19–31. https://doi.org/10.1007/s10750-009-9981-8

Osborn, R., Dillon, B., Tran, D., Abolfazli, E., Dunne, K. B. J., Nittrouer, J. A., & Strom, K. (2021). FlocARAZI: An in-situ, image-based profiling instrument for sizing solid and flocculated suspended sediment. *Journal of Geophysical Research: Earth Surface*, *126*(11), e2021JF006210. https://doi.org/10.1029/2021jf006210

Parsons, D. R., Schindler, R. J., Hope, J. A., Malarkey, J., Baas, J. H., Peakall, J., et al. (2016). The role of biophysical cohesion on subaqueous bed form size. *Geophysical Research Letters*, *43*(4), 1566–1573. https://doi.org/10.1002/2016gl067667

Payne, J. T., Jackson, C. R., Millar, J. J., & Ochs, C. A. (2020). Timescales of variation in diversity and production of bacterioplankton assemblages in the Lower Mississippi River. *PLoS One*, *15*(4), e0230945. https://doi.org/10.1371/journal.pone.0230945

Phillips, J. M., & Walling, D. E. (1999). The particle size characteristics of fine-grained channel deposits in the River Exe Basin, Devon, UK. *Hydrological Processes*, *13*(1), 1–19. https://doi.org/10.1002/(sici)1099-1085(199901)13:1<1::aid-hyp674>3.0.co;2-c

Rouse, H. (1939). *An analysis of sediment transportation in the light of fluid turbulence* (Tech. Rep. No. SCS-TR 25). U.S. Department of Agriculture, Soil Conservation Service.

Schieber, J., Southard, J. B., & Thaisen, K. (2007). Accretion of mudstone beds from migrating floccule ripples. *Science*, *318*(5857), 1760–1763. https://doi.org/10.1126/science.1147001

Smith, S. J., & Friedrichs, C. T. (2011). Size and settling velocities of cohesive flocs and suspended sediment aggregates in a trailing suction hopper dredge plume. *Continental Shelf Research*, *31*(10), S50–S63. https://doi.org/10.1016/j.csr.2010.04.002

Spearman, J. R., Manning, A., & Whitehouse, R. J. (2011). The settling dynamics of flocculating mud and sand mixtures: Part 2—Numerical modelling. *Ocean Dynamics*, *61*(2–3), 351–370. https://doi.org/10.1007/s10236-011-0385-8

Spencer, K. L., Wheatland, J. A., Carr, S. J., Manning, A. J., Bushby, A. J., Gu, C., et al. (2022). Quantification of 3-dimensional structure and properties of flocculated natural suspended sediment. *Water Research*, *222*, 118835. https://doi.org/10.1016/j.watres.2022.118835

Spencer, K. L., Wheatland, J. A. T., Bushby, A. J., Carr, S. J., Droppo, I. G., & Manning, A. J. (2021). A structure–function based approach to floc hierarchy and evidence for the non-fractal nature of natural sediment flocs. *Scientific Reports*, *11*(1), 14012. https://doi.org/10.1038/s41598-021-93302-9

Strom, K., & Keyvani, A. (2011). An explicit full-range settling velocity equation for mud flocs. *Journal of Sedimentary Research*, *81*(12), 921–934. https://doi.org/10.2110/jsr.2011.62

Strom, K., Osborn, R., Dunne, K. B. J., & Nittrouer, J. A. (2023). Suspended particle and floc sizes in the lower most reaches of the Mississippi River during summer 2020 and winter 2021 (v1.0.0) [Dataset]. Zenodo. https://doi.org/10.5281/zenodo.7826382

Tambo, N., & Hozumi, H. (1979). Physical characteristics of flocs-II: Strength of floc. *Water Research*, *13*(5), 421–427. https://doi.org/10.1016/0043-1354(79)90034-4

Tan, X., Hu, L., Reed, A., Furukawa, Y., & Zhang, G. (2013). Flocculation and particle size analysis of expansive clay sediments affected by biological, chemical, and hydrodynamic factors. *Ocean Dynamics*, *64*, 1–15. https://doi.org/10.1007/s10236-013-0664-7

Thill, A., Moustier, S., Garnier, J.-M., Estournel, C., Naudin, J.-J., & Bottero, J.-Y. (2001). Evolution of particle size and concentration in the Rhône river mixing zone: Influence of salt flocculation. *Continental Shelf Research*, *21*(18), 2127–2140. https://doi.org/10.1016/s0278-4343(01)00047-4

Tran, D., & Strom, K. (2017). Suspended clays and silts: Are they independent or dependent fractions when it comes to settling in a turbulent suspension? *Continental Shelf Research*, *138*, 81–94. https://doi.org/10.1016/j.csr.2017.02.011

Turner, R. E., Milan, C. S., Swenson, E. M., & Lee, J. M. (2022). Peak chlorophyll a concentrations in the lower Mississippi River from 1997 to 2018. *Limnology & Oceanography*, *67*(3), 703–712. https://doi.org/10.1002/lno.12030

Uncles, R. J., Bale, A. J., Stephens, J. A., Frickers, P. E., & Harris, C. (2010). Observations of floc sizes in a muddy estuary. *Estuarine, Coastal and Shelf Science*, *87*(2), 186–196. https://doi.org/10.1016/j.ecss.2009.12.018

Van der Lee, W. T. B. (2000). Temporal variation of floc size and settling velocity in the Dollard estuary. *Continental Shelf Research*, *20*(12–13), 1495–1511. https://doi.org/10.1016/s0278-4343(00)00034-0

van Leussen, W. (1994). *Estuarine macroflocs and their role in fine-grained sediment transport* (Unpublished doctoral dissertation). University of Utrecht, .

Van Prooijen, B. C., & Winterwerp, J. C. (2010). A stochastic formulation for erosion of cohesive sediments. *Journal of Geophysical Research*, *115*(C1), C01005. https://doi.org/10.1029/2008jc005189

Verney, R., Lafite, R., & Brun-Cottan, J.-C. (2009). Flocculation potential of estuarine particles: The importance of environmental factors and of the spatial and seasonal variability of suspended particulate matter. *Estuaries and Coasts*, *32*(4), 678–693. https://doi.org/10.1007/s12237-009-9160-1

Whitehouse, R. J. S., Soulsby, R., Robert, W., & Mitchener, H. (2000). *Dynamics of estuarine muds: A manual for practical applications*. Thomas Telford.

Wiberg, P. L., Law, B. A., Wheatcroft, R. A., Milligan, T. G., & Hill, P. S. (2013). Seasonal variations in erodibility and sediment transport potential in a mesotidal channel-flat complex, Willapa Bay, {WA}. *Continental Shelf Research*, *60*, S185–S197. https://doi.org/10.1016/j.csr.2012.07.021

Winterwerp, J. C. (1998). A simple model for turbulence induced flocculation of cohesive sediment. *Journal of Hydraulic Research*, *36*(3), 309–326. https://doi.org/10.1080/00221689809498621

Winterwerp, J. C., & van Kesteren, W. G. M. (2004). *Introduction to the physics of cohesive sediment in the marine environment* (Vol. 56). Elsevier.

Woodward, J. C., & Walling, D. E. (2007). Composite suspended sediment particles in river systems: Their incidence, dynamics and physical characteristics. *Hydrological Processes*, *21*(26), 3601–3614. https://doi.org/10.1002/hyp.6586

Wright, S., & Parker, G. (2004a). Density stratification effects in sand-bed rivers. *Journal of Hydraulic Engineering*, *130*(8), 783–795. https://doi.org/10.1061/(asce)0733-9429(2004)130:8(783)

Wright, S., & Parker, G. (2004b). Flow resistance and suspended load in sand-bed rivers: Simplified stratification model. *Journal of Hydraulic Engineering*, *130*(8), 796–805. https://doi.org/10.1061/(asce)0733-9429(2004)130:8(796)